TECHNOLOGY FORCES

Journal of Engineering and Sciences

ISSN 1994-862X (Print)
ISSN 2790-0053 (Electronic)

Volume 5 - Issue 01 | January - June 2023

KIET Research Projects

KIET

Karachi Institute of Economics & Technology

Technology Forces

Journal of Engineering and Sciences

EDITORIAL BOARD

College of Engineering
Karachi Institute of Economics & Technology

COLLEGE OF ENGINEERING

Vision

"To impart highest quality engineering education with an aim to produce proficient, creative and ethical engineers who can take the role of visionary leaders, entrepreneurs and researchers at national and global levels".

Mission

"To educate students through highly qualified faculty to have strong theoretical and practical expertise, team-work, leadership qualities, ethical values and entrepreneurship skills. Establish and maintain state-of-the-art laboratories, latest curriculum and industrial linkages. Prepare graduates to pursue higher studies and undertake research at national and global levels".

AIMS AND SCOPE

Technology Forces Journal is a peer-reviewed journal that aims at the publication and dissemination of original research articles on the latest developments in all fields of engineering, science and technology. The journal publishes original papers in English which contribute to the understanding of engineering science and improvement of the engineering technology and education. Papers may be theoretical (including computational), experimental or both. The contribution should be unpublished before and not under consideration for publication elsewhere. Technology Forces Journal maintains a standard double-blind peer review process. The double-blind process means that the identity of the author and the reviewer are not known to each other.

Focused areas for publication include, but not limited to:

- Signal Processing
- Data Mining and Visual Analytics
- Software Engineering & Future Generation Computing
- Emnedded Systems
- Smart Networks
- Molecular and Nanoelectronics
- Applied Controls and Power

OPEN ACCESS POLICY

For the benefit of authors and research community, this journal adopts open access policy, which means that the authors can self-archive their published articles on their own website or their institutional repositories. The readers can download or reuse any article free of charge for research, further study or any other non-profitable academic activity.

PEER REVIEW POLICY

Peer review is the process to uphold the quality and validity of the published articles. Technology Forces Journal uses double-blind peer review policy to ensure only high-quality publications are selected for the journal. Paper are referred to at least two experts as suggested by the editorial board. All publication decisions are made by the journal's Editors-in-Chief on the basis of the referees' reports. We expect our board of reviewing editors and reviewers to treat manuscripts as confidential material. The identitites of the authors and reviewers remain confidential throughout the process.

COPYRIGHT

DISCLAIMER

The opinions expressed in Technology Forces Journal are those of the authors and contributors, and do not necessarily reflect those of the journal management, adviosory board and the editorial board Paper published in Technology Forces Journal are processed through double blind peer-review by subject specialists and language expert. Neither the College of Engineering and nor the editors of Technology Forces Journal can be held responsible for errors or any consequences arising from the use of information contained in the journal, instead, errors should be reported directly to the corresponding authors of the articles.

TABLE OF CONTENTS

A Numerical PID Tuning Approach for LTI Systems

Talha Asif
GIK Institute of Engineering Sciences & Technology
Topi, Pakistan
gee2048@giki.edu.pk

Salman Zaffar
Independent Researcher
salmanfar@gmail.com

Abstract—This paper presents a novel PID tuning approach for n[th]-order LTI systems. It is a purely time-domain approach which determines the controller gains k_P, k_I, and k_D by utilizing the characteristic polynomial of closed-loop output dynamics. Using the fact that the value of discriminant of the characteristic polynomial of output dynamics is representative of critically-, under- or over-damped transient response, the proposed numerical approach computationally searches for those sets of controller gains which yield the desired transient response. Furthermore, the computational search can be refined by considering step response attributes such as rise time, settling time, overshoot and etc. Simulation results are included to show the efficacy of the proposition.

Index Terms—LTI systems, Linear Control Design, Numerical PID Tuning, Output Dynamics Polynomial Discriminant, Control

I. Introduction

PID control is the most popular approach in industrial control applications [1]. LTI systems with PID control are mathematically represented by non-homogeneous linear ODEs. Traditionally, a PID control design involves two steps, i.e., (i) Laplace Transform is used to convert such ODEs to s-domain and (ii) application of various PID tuning algorithms such as manual tuning, Ziegler Nichols [2], Tyreus Luyben, Cohen–Coon [3], or Astr˚om-H¨ agglund [1] etc. for determination¨ of controller gains k_P, k_I, and k_D. The novelty in this paper is that the proposed PID tuning approach is (i) time-domain, and (ii) numerical. It is demonstrated through simulations that the proposed numerical approach is applicable to n^{th}-order LTI systems.

Higher-order LTI plants can be used for modeling applications in aircraft, cement, chemical, flexible robot manipulator [4], fuel injectors [6], nuclear plants, oil, pharmaceutical, quadcopter with a variable degree of freedom (DOF) [5]. Many of these plants are nonlinear plants and turn out as higher-order LTI plants when linearized at an operating point [7], [8]. Also, modeling of plants through the finite-element model or the first principle leads to higher-order plants [9], [10]. Control of higher-order LTI systems is not a trivial task because the system complexity may result in ill-conditioning making computations impractical due to memory and time limitations [11]. If the order of the system is more than two, it is referred to as a higher-order control system [12].

PID control with minimum computational expenditure can be applied on higher-order systems by utilizing model reduction methods. Model reduction methods are employed to replace a higher-order system with its lower-order approximation. These methods include model reduction by impulse/step error minimization, Routh approximation techniques, principal component analysis method [14], Pade approximation methods, and balanced-truncation method [15]. In 2011, a fractional order controller with a model reduction method for higher order systems was proposed by S. Das et al. [9]. In 2014, a fuzzy self-tuning PID controller for higher-order systems was proposed by RituRani et al. [13]. These reduced models are required to contain the essence of the characteristics of the original system, however, it is not always possible to have these characteristics completely. Hence, the reduced order model is not pertinent to all applications, if it is not acquiring important characteristics. The disadvantage of some of the methods mentioned above is that they do not guarantee stable reduced models even though the original system is stable. In this paper, a higher-order system is designed using the PID controller without using model reduction techniques.

As for the time-domain based PID control approaches, one of the main time-domain based PID control approaches is Eigenvalue assignment [16]. Performance of a closed-loop system is directly related to the eigenvalues of the system. However, in case gains that would at least yield the dominant eigenvalues for a desired performance, a generalization of Hermite-Biehler theorem has been used in [17] for controller design. This theorem gives a necessary and sufficient condition to render a given real polynomial in the sense of Hurwitz stability.

The contribution in this paper is based on the fact that the gains kP, kI, and kD of a closed-loop system become the coefficients of the characteristic polynomials of output and zero dynamics. It is known that two dominant eigenvalues of the output dynamics characteristic polynomial determine the nature of the transient response. The response can be over-, critically- or under-damped when the two dominant eigenvalues are real and distinct, real and equal or a complex conjugate pair, respectively. The discriminant Δ of an output dynamics characteristic polynomial can also be used to determine the nature of transient response, i.e., $\Delta > 0$, $\Delta = 0$, or $\Delta < 0$ resulting respectively in over-, critically-, or under-damped transient response. Analytical calculation of Δ for 1st- and 2nd-order systems are possible but numerical calculation of Δ is required in case of higher-order systems. The main contribution in this paper is that the Δ is calculated numerically to achieve the desired transient response. This numerical approach utilizes the determinant of the Sylvester matrix, which is formed by the output dynamics characteristic polynomial. The use of the Sylvester matrix can also be found in [19], [20].

The sections below are organised in the following manner. Some preliminary concepts are shown in Section II to better understand the problem statement presented in Section III. In Section IV, the main result of this paper is presented. Section V elaborates the main result in Section IV. Section VI uses a motivating example, taken from [16], on which the proposed numerical approach is applied. Section VII presents the simulation results obtained from applying the proposed numerical approach on the motivating example.

II. PRELIMINARIES

In order to present the problem statement few preliminary concepts need to be understood. Consider the following generic open-loop differential equation of an LTI plant

$$a_n y_n + a_{n-1} y_{n-1} + a_{n-2} y_{n-2} + \cdots + a_1 y_0 + a_0 y(t) = b_n u_n +$$

$$b_{n-1} u_{n-1} + b_{n-2} u_{n-2} + \cdots + b_1 u_0 + b_0 u(t).$$

(1)

In the equation above, the open-loop output dynamics expression is defined as

$$a_n y_n + a_{n-1} y_{n-1} + a_{n-2} y_{n-2} + \cdots + a_1 y_0 + a_0 y(t)$$

(2)

and the open-loop zero dynamics expression in Equation (1) is given by

$$b_n u^n + b_{n-1} u^{n-1} + b_{n-2} u^{n-2} + \cdots + b_1 u' + b_0 u(t). \quad (3)$$

The input u(t) to the open-loop plant in Equation (1) is the output of the PID controller defined by

$$u(t) = K_P e(t) + K_I \quad e(t)dt + K_D e\,(t)$$

where the error is calculated as the difference of a reference input applied to the system and the output of the system, i.e., e(t) = r(t) − y(t). The closed-loop differential equation is obtained by applying Equation (4) into Equation (1) and by substituting e(t) = r(t) − y(t). The closed-loop differential equation, depending upon the type of controller, i.e., either P, PI, PD or PID, applied at the input u(t), is generalized by

$$c_m y_m + c_{m-1} y_{m-1} + c_{m-2} y_{m-2} + \cdots + c_1 y_0 + c_0 y(t) = d_m r_m +$$

$$d_{m-1} r_{m-1} + d_{m-2} r_{m-2} + \cdots + d_1 r_0 + d_0 r(t)$$

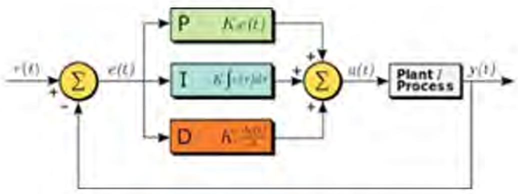

Fig. 1. Closed Loop System with PID Controller

where the closed-loop zero dynamics expression in Equation (5) is given as

$$R = d_m r_m + d_{m-1} r_{m-1} + d_{m-2} r_{m-2} + \cdots + d_1 r_0 + d_0 r(t)$$

and the closed-loop output dynamics expression and its first derivative of Equation (5) are defined as

$$Y = c_m y^m + c_{m-1} y^{m-1} + \cdots + c_1 y^0 + c_0 y(t)$$

$$Y^{'} = m c_m y^{m-1} + (m-1) c_{m-1} y^{m-2} + \cdots + c_1 y(t)$$

where $Y^{'} = \frac{dY}{dy}$. The characteristic polynomial of the output dynamics expression in Equation (7) is expressed below

$$c_m s^m + c_{m-1} s^{m-1} + \cdots + c_1 s + c_0$$

where m is the degree of the polynomial and the coefficients $c_m, \cdots, c_0$ are generally functions of plant parameters an,··· ,a0 and $b_n, \cdots, b_0$ in Equation (1) and controller gains k_P, k_I, and k_D. The generalized resulting block diagram of the closed-loop system is shown in Figure 1, which is taken from [21].

III. Problem statement

Generally, the discriminant of the characteristic polynomial in Equation (8) can be used to determine the transient response of the system. In case of a first-order plant controlled with a P, PI, PD or PID controller, the degree of the characteristic polynomial of the output dynamics will not be higher than 2. Discriminant of a quadratic equation is easily determinable and thus analytically solvable resulting in values of the individual gains kP,kI and kD depending on the desired transient response, i.e., under-damping $\Delta < 0$ or over-damping $\Delta > 0$, or critical-damping $\Delta = 0$. In case of an n^{th}-order plant controlled with a P or PD controller, the degree of the characteristic polynomial will be n and controlled with a PI or PID controller, the degree of the characteristic polynomial will be n+1. In such cases it is harder to find the discriminant let alone solve analytically for k_P, k_I, and k_D.

In this paper, we employ a numerical solution for discriminant calculation by iteratively searching for controller gains k_P, k_I, and k_D for desired transient response. The proposed numerical approach is summarized in the next section.

Algorithm Generic PID Tuning

Input: $a_n, a_{n-1}, a_{n-2}, \cdots, a_1, a_0$
Input: $b_n, b_{n-1}, b_{n-2}, \cdots, b_1, b_0$
Input: k_{Pmin}, k_{Imin}, k_{Dmin}
Input: k_{Pmax}, k_{Imax}, k_{Dmax} Input: Δ_{min},
Δ_{max} for $k_P \leftarrow k_{Pmin}$ *to* k_{Pmax} do for $k_I \leftarrow$
k_{Imin} *to* k_{Imax} do for
$k_D \leftarrow k_{Dmin}$ *to* k_{Dmax} do
$Res(Y, Y^{'}) \leftarrow |S_{Y,Y^{'}}|$
$\Delta \leftarrow \frac{-1^{\frac{m(m-1)}{2}}}{c_m} Res(Y, Y^{'})$
if $\Delta_{min} < \Delta < \Delta_{max}$ then if
k_P 6= 0 then
print Δ, k_P, k_I, k_D print Zero dynamics
Eigenvalues print Output dynamics
Eigenvalues print Step Response
Attributes end if
end if
end for end
for
end for

IV. Main result

The aforementioned numerical approach being the main result is given in the form of an algorithm that determines the gains k_P, k_I, and k_D for a PID controlled LTI system. A few important concepts need to be addressed for better understanding the algorithm. The discriminant is numerically calculated as given below

$$\Delta = \frac{-1^{\frac{m(m-1)}{2}}}{c_m} Res(Y, Y^{'})$$

(9)

where the resultant of Y and its first derivative Y' from Equation (7) is given by the determinant of the Sylvester matrix of Y and its first derivative Y'

$$Res(Y, Y') = |S_{YY'}|.$$

The factor $S_{Y,Y'}$ is the Sylvester matrix of Y and Y'. Sylvester matrix is square having size $(2m - 1)$, where m is the degree of the characteristic polynomial in Equation (8).

This matrix is formed as

$$\begin{pmatrix} c_m & c_{m-1} & & \cdots & c_0 & 0 & \cdots & 0 \\ 0 & c_m & c_{m-1} & & \cdots & c_0 & 0 & \cdots \\ \vdots & & \ddots & & & & & \\ 0 & \cdots & & & c_m & c_{m-1} & \cdots & c_0 \\ mc_m & (m-1)c_{m-1} & & \cdots & c_1 & 0 & \cdots & 0 \\ 0 & mc_m & (m-1)c_{m-1} & & \cdots & c_1 & 0 & \cdots \\ \vdots & & \ddots & & & & & \\ 0 & \cdots & & & mc_m & (m-1)c_{m-1} & \cdots & c_1 \end{pmatrix} \quad (11)$$

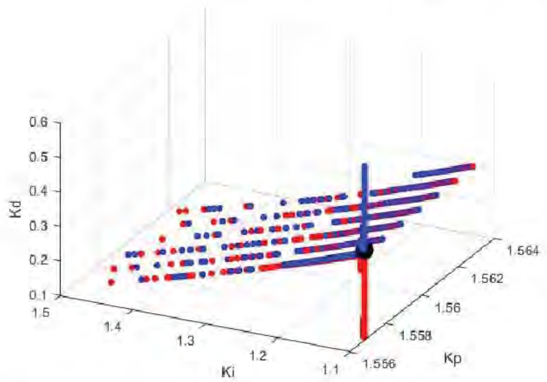

Fig. 2. Over- and Under-damped Transient Responses at Different Values of the Controller Gains. Blue Points Represent Under-damped Response whereas Red Points Represent Over-damped Response.

V. Explanation

This algorithm first prompts the user to specify the openloop output dynamics expression and zero dynamics expression coefficients in Equation (1). The number of coefficients of each expression enables the proposed algorithm to identify the order of the plant. Then the algorithm prompts the user to specify the minimum and maximum values of controller gains k_P, k_I, and k_D and Δ. The range stated by the values of Δ min and Δmax specify which type of transient response is required. If the desired transient response is over-damped, then the values of Δmin and Δmax should both be greater than zero. If the desired transient response is under-damped, then the values of Δ min and Δmax should both be less than zero. If the desired response is critically-damped, then the value of Δmin should be less than zero and the value of Δ max should be greater than zero, and both the values should be as close to zero as possible.

During each iteration the open-loop plant becomes closed-loop using the current values of the controller gains k_P, k_I, and k_D. Then the numerical discriminant of Equation (8) is calculated, which is simply the quotient of the resultant and the first coefficient of the characteristic polynomial cm. The first if condition checks whether the calculated discriminant lies within the range specified. If so then the results are returned to the user. The second if condition discards all cases where the controller gain kP is zero as an Integral-Derivative controller is not preferred due to various problems such as stability.

As far as the result of the algorithm is concerned, each iteration ends with return of the current values of discriminant, respective controller gains k_P, k_I, and k_D, zero dynamics eigenvalues, output dynamics eigenvalues and step response attributes. Step response attributes contain information about the rise time, settling time, steady-state error, maximum overshoot and undershoot. Thus, the user may select the best possible transient response.

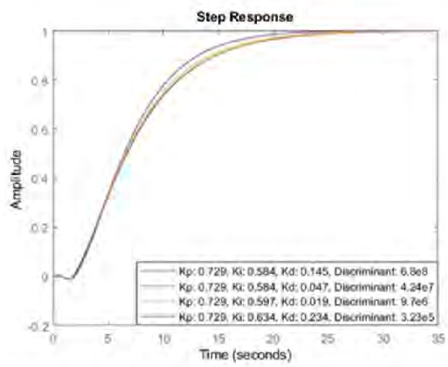

Fig. 3. Over-damped Transient Response with Respect to Positive Values of Discriminant

The desired transient response is not achieved if the zero dynamics eigenvalues dominate the output dynamics eigenvalues. This is due to the fact that the dominant zero dynamics eigenvalues will decrease the rise time of the transient response. Thus, the user may select a transient response with less dominant zero dynamics eigenvalues.

To specifically target the results of a P, PI or PD controller, the maximum and minimum values of the unnecessary individual gains be set to zero. For example to obtain results for a closed-loop plant controlled with a P controller, then the minimum and maximum values of the gains k_I, and k_D be set to zero. So in such a case the algorithm will function having a single for loop, to iterate the value of the gain k_P.

VI. Motivating Example

Consider an open-loop differential equation of an LTI plant whose transfer function form is reported in [16]. The openloop transfer function and differential equation are shown below

$$G(s) = \frac{-0.1s^3 + s^2 - 3.3s + 3.6}{s^5 + 5s^4 + 22s^3 + 46s^2 + 46s + 17}$$

$$y^{V} + 5y^{IV} + 22y^{ooo} + 46y^{oo} + 46y^{o} + 17y(t) =$$

$$-0.1u''' + u'' - 3.3u' + 3.6u(t)$$

When PID controller is applied to Equation (13), the closed loop differential equation, having the form of Equation (5), is obtained which is further converted to controllable canonical state-space representation as shown below

$$\dot{x}(t) = Ax(t) + Br(t)$$
$$y = Cx(t)$$

$$A = \begin{pmatrix} 0 & 1 & 0 & 0 & 0 & 0 \\ 0 & 0 & 1 & 0 & 0 & 0 \\ 0 & 0 & 0 & 1 & 0 & 0 \\ 0 & 0 & 0 & 0 & 1 & 0 \\ 0 & 0 & 0 & 0 & 0 & 1 \\ -c_0 & -c_1 & -c_2 & -c_3 & -c_4 & -c_5 \end{pmatrix} \quad (14)$$

$$B = \begin{pmatrix} 0 \\ 0 \\ 0 \\ 0 \\ 0 \\ 1 \end{pmatrix}$$

$$C = (d_0 \quad d_1 \quad d_2 \quad d_3 \quad d_4 \quad d_5)$$

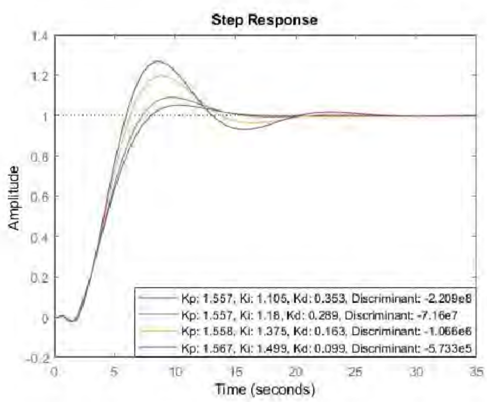

Fig. 4. Under-damped Transient Response with Respect to Negative Values of Discriminant

The Sylvester matrix of the system in Equation (14) is generalized for this motivating example by a 11 × 11 square matrix. Since the degree of the characteristic polynomial in Equation (14) is of the value $m = 6$, so $2m - 1 = 11$. The square matrix is formed as shown below

$$\begin{pmatrix} c_6 & c_5 & c_4 & c_3 & c_2 & c_1 & c_0 & 0 & 0 & 0 & 0 \\ 0 & c_6 & c_5 & c_4 & c_3 & c_2 & c_1 & c_0 & 0 & 0 & 0 \\ 0 & 0 & c_6 & c_5 & c_4 & c_3 & c_2 & c_1 & c_0 & 0 & 0 \\ 0 & 0 & 0 & c_6 & c_5 & c_4 & c_3 & c_2 & c_1 & c_0 & 0 \\ 0 & 0 & 0 & 0 & c_6 & c_5 & c_4 & c_3 & c_2 & c_1 & c_0 \\ 6c_6 & 5c_5 & 4c_4 & 3c_3 & 2c_2 & c_1 & 0 & 0 & 0 & 0 & 0 \\ 0 & 6c_6 & 5c_5 & 4c_4 & 3c_3 & 2c_2 & 0 & 0 & 0 & 0 & 0 \\ 0 & 0 & 6c_6 & 5c_5 & 4c_4 & 3c_3 & 2c_2 & 0 & 0 & 0 & 0 \\ 0 & 0 & 0 & 6c_6 & 5c_5 & 4c_4 & 3c_3 & 2c_2 & 0 & 0 & 0 \\ 0 & 0 & 0 & 0 & 6c_6 & 5c_5 & 4c_4 & 3c_3 & 2c_2 & 0 & 0 \\ 0 & 0 & 0 & 0 & 0 & 6c_6 & 5c_5 & 4c_4 & 3c_3 & 2c_2 & c_1 \end{pmatrix}$$

Consider the case when the controller applied to the openloop plant in Equation (13) is a PID controller then the values of the coefficients in Equation (14) and (15) are listed below

$c_6 = 1$	$d_5 = -0.1k_D$
$c_5 = 5 - 0.1k_D$	$d_4 = k_D - 0.1k_P$
$c_4 = 22 + k_D - 0.1k_P$	$d_3 = -3.3k_D + k_P - 0.1k_I$
$c_3 = 46 - 3.3k_D + k_P - 0.1k_I$	$d_2 = 3.6k_D - 3.3k_P + k_I$
$c_2 = 46 + 3.6k_D - 3.3k_P + k_I$	$d_1 = 3.6k_P - 3.3k_I$
$c_1 = 17 + 3.6k_P - 3.3k_I$	$d_0 = 3.6k_I$
$c_0 = 3.6k_I$	

Note the columns of this aforementioned matrix in Equation (15) are all linearly independent. It can be confirmed by applying row-reduction on the matrix as the resulting matrix is an 11×11 identity matrix. The conclusions that can be drawn here are enumerated below

1) the discriminant will never be equal to zero by Equation (9) unless any two columns or two rows are identical. Identical columns or rows render the determinant of a matrix zero. Generalizing this idea to the matrix in Equation (11), it can be said that the critical-damping is never achievable by a PID controller.
2) the controller gains k_P, k_I, and k_D cannot make the system of this motivating example critically-damped both in theory as well as in practice.

TABLE I

Values of Discriminant, Output Dynamics Eigenvalues and Zero Dynamics Eigenvalues Against 4 Sets of Controller Gains for Over-damped Response

Controller Gains	Δ	Output Dynamics Eigenvalues	Zero Dynamics Eigenvalues
Kp: 0.729 Ki: 0.584 Kd: 0.145	6.802×10^{8}	-0.2033 -0.5491 $-1.0008\pm3.4410i$ $-1.1157\pm0.4708i$	4 3 3 -1 -4.0276
Kp: 0.729 Ki: 0.584 Kd: 0.047	4.235×10^{7}	-0.1997 -0.6648 $-0.9796\pm3.4375i$ $-1.0858\pm0.2465i$	4 3 3 -0.8474 -14.6632
Kp: 0.729 Ki: 0.597 Kd: 0.019	9.703×10^{6}	-0.2106 -0.6612 $-0.9735\pm3.4364i$ $-1.0897\pm0.1495i$ -	4 3 3 -0.8372 -37.5312
Kp: 0.729 Ki: 0.634 Kd: 0.234	3.229×10^{5}	0.3231 -0.3262 $-1.0197\pm3.4441i$ $-1.1439\pm0.6080i$	4 3 3 -1.5577 $\pm0.5320i$

VII. Simulation Results

This section presents the simulation results achieved by applying the proposed numerical PID tuning approach on the motivating example of [16]. As a reference, the two reported controller gains in [16], which are also obtained through the proposed numerical approach are tabulated after

TABLE II

Transient Responses and Respective Controller Gains of [16]

Response	k_P	k_I	k_D
Over-Damped	0.729	0.584	0.047
Under-Damped	1.557	1.105	0.353

The first step in applying the proposed numerical approach involves the specification of ranges for controller gains and discriminant. The controller gains ranges from k_P : 1.55 to 2, k_I : 1 to 1.5 and k_D : 0 to 0.5 for under-damped response and from k_P : 0.7 to 1, k_I : 0.5 to 1 and k_D : 0 to 0.5 for overdamped response. The discriminant ranges from 1 × 109 to 0 for over-damped response and from 0 to −1×109 for underdamped response. The step size for controller gains increment within respective ranges is 0.001.

The first step in applying the proposed numerical approach involves the specification of ranges for controller gains and discriminant. The controller gains ranges from k_P : 1.55 to 2, k_I : 1 to 1.5 and k_D : 0 to 0.5 for under-damped response and from k_P : 0.7 to 1, k_I : 0.5 to 1 and k_D : 0 to 0.5 for overdamped response. The discriminant ranges from 1 × 109 to 0 for over-damped response and from 0 to −1×109 for underdamped response. The step size for controller gains increment within respective ranges is 0.001.

TABLE III

Values of Discriminant, Output Dynamics Eigenvalues and Zero Dynamics Eigenvalues Against 4 Sets of Controller Gains for Under-damped Response

Controller Gains	Δ	Output Dynamics Eigenvalues	Zero Dynamics Eigenvalues
Kp: 1.557 Ki: 1.105 Kd: 0.353	-2.209×10^{8}	$-0.3325\pm0.3486i$ $-1.0157\pm3.4883i$ $-1.1342\pm0.1102i$	4 3 3 -0.8888 -3.5220
Kp: 1.557 Ki: 1.18 Kd: 0.289	-7.160×10^{7}	$-0.2930\pm0.3765i$ $-1.0015\pm3.4845i$ $-1.1911\pm0.0385i$	4 3 3 -0.9124 -4.4752
Kp: 1.558 Ki: 1.375 Kd: 0.163	-1.066×10^{6}	$-0.2209\pm0.4202i$ $-0.9732\pm3.4773i$ $-1.2977\pm0.0021i$	4 3 3 -0.9838 -8.5745
Kp: 1.567 Ki: 1.499 Kd: 0.099	-5.733×10^{5}	$-0.1883\pm0.4394i$ $-0.9584\pm3.4743i$ $-1.3483\pm0.0011i$	4 3 3 -1.0227 -14.8056

point, just next to critical damping, as the two dominant eigenvalues are real and approximately equal.

As for the simulation results for under-damped scenario, values of discriminant vary in a negative range. A smaller value of discriminant in this range, $\Delta = -2.209 \times 10^{8}$, induces weak under-damping characterized by larger rise time, smaller settling time and smaller overshoot. As the value of discriminant increases in the negative range, under-damping becomes stronger characterized by smaller rise time, larger settling time and larger overshoot. Figure 4 shows the underdamped transient response with respect to negative values of discriminant. Moreover, Table *III* tabulates the values of discriminant, output dynamics eigenvalues and zero dynamics eigenvalues against four sets of controller gains. It is noticeable that a negative discriminant for all the four sets of controller gains render the dominant output dynamics eigenvalues a complex conjugate pair thereby resulting in an under-damped transient response.

It has been shown in this paper that the values of controller gains finely control the value of the discriminant. Thus, it can be expected that the transient response is also finely dependent upon the values of controller gains. For controller gains ranges k_P : 1.55 to 2, k_I : 1 to 1.5 and k_D : 0 to 0.5, Figure 2 shows the over- and under-damped transient responses. Blue points represent under-damped response whereas red points represent over-damped response. The big black point represents an under-damped response reported in [16] and Table *II*.

The first step in applying the proposed numerical approach involves the specification of ranges for controller gains and discriminant. The controller gains ranges from k_P : 1.55 to 2, k_I : 1 to 1.5 and k_D : 0 to 0.5 for under-damped response and from k_P : 0.7 to 1, k_I : 0.5 to 1 and k_D : 0 to 0.5 for overdamped response. The discriminant ranges from 1 × 109 to 0 for over-damped response and from 0 to −1×109 for underdamped response. The step size for controller gains increment within respective ranges is 0.001.

REFERENCES

1. Astr˚om, K. J., & H¨ agglund, T. (2006). Advanced PID control. In Re-¨ search triangle park: Instrumentation, systems, and automation society.
2. J. G. Ziegler and N.B. Nichols, Optimum Settings for Automatic Controllers. Trans. ASME. 64(8): p. 759–768, 1942.
3. G. H. Cohen and G. A. Coon, Theoretical Consideration of Retarded Control. Trans. ASME. 75: p. 827– 834, 1953.
4. V. Azimi, M. B. Menhaj and A. Fakharian, Tool position tracking control of a nonlinear uncertain flexible robot manipulator by using robust H2/H controller via T–S fuzzy model, Sadhana 40, 307–333 (2015).
5. O.¨ Urlu¨,¨ V. Emre, U. Bu¨yu¨ks¸ahin, R. Artar, A. Kirli and T. M. Nurullah, An experimental stationary quadrotor with variable DOF,Sadhana 38, 247–264 (2013).
6. S. N. Deepa and G. Sugumaran, Design of PID controller for higher order continuous systems using MPSO based model formulation technique, Int. J. Electr. Electron. Eng. 5, 289–295 (2011).
7. K. Hassan and J. W. Grizzle, Nonlinear Systems, 3, Prentice Hall, Upper Saddle River, 2002.
8. S. Saha, S. Das, R. Ghosh, B. Goswami, R. Balasubramanian, A. K. Chandra, S. Das and A. Gupta, Design of a fractional order phase shaper for iso-damped control of a PHWR under step-back condition, Nucl. Sci. IEEE Trans. 57, 1602–1612 (2010).
9. S. Das, S. Saha, S. Das and A. Gupta, On the selection of tuning methodology of FOPID controllers for the control of higher order processes, ISA Transact. 50, 376–388 (2011).
10. MATHWORKS, Simplifying higher-order plant models http://in.mathworks.com/help/robust/examples/ simplifying-higher-order-plant-models.ht, 2008.
11. S. D. Jukic´, A. T. Saric´, dynamics model reduction: An overview of available techniques with application to power systems, Serbian J. Electr. Eng. 9, 131–169 (2012).
12. K. Ogata and Y. Yang, Modern Control Engineering, Prentice-Hall, Englewood Cliffs, 1970.
13. R. De Maity and R. Mudi, Fuzzy Self-tuning of Conventional PID Controller for High-Order Processes, vol. 247 of Advances in Intelligent Systems and Computing, Springer International Publishing, 2014.
14. B. Moore, Principal component analysis in linear systems: Controllability, observability, and model reduction, Automat. Contr. IEEE Trans. 26(1), 17-32 (1981).
15. M. Safonov and R. Chiang, A Schur method for balanced-truncation model reduction, Automatic Contr. IEEE Transact. 34 (7) , 729-733
16. (1989).
17. Jianchang Liu, Honghai Wang, Yu Zhang, New result on PID controller design of LTI systems via dominant eigenvalue assignment, Automatica, Volume 62, 2015, Pages 93-97, ISSN 0005-1098, https://doi.org/10.
18. 1016/j.automatica.2015.09.009.
19. Gantmacher, (1959). The theory of matrices. New York: Chelsea.
20. Golnaraghi, F., & Kuo, B. C. (2010). Automatic control systems (9th ed.). John Wiley & Sons, INC.
21. V. Kucera. Diophantine Equations in Control–A Survey. Automatica, 29:6:1361-1375, 1993.
22. K.J. Astr˚ om, B. Wittenmark. Computer–Controlled Systems, Theory and¨ Design. Prentice Hall, Information and Systems Sciences Series, 1997, 186-195.
23. https://commons.wikimedia.org/wiki/File:PID.svg

CONTROL OF ROBOTIC ARM MANIPULATOR JOINT

Muhammad Talha
Dept of Mechanical and Aerospace Engineering
Air University, Islamabad, Pakistan
200520@students.au.edu.pk

Faizan Ali
Dept of Mechanical and Aerospace Engineering
Air University, Islamabad, Pakistan
200512@students.au.edu.pk

Dr. Syed Irtiza Ali Shah
Dept of Mechanical and Aerospace Engineering
Air University, Islamabad, Pakistan
irtiza@mail.au.edu.pk

Engr. Majid Mehmood
Dept of Mechanical and Aerospace Engineering
Air University, Islamabad, Pakistan
majid.25mehmood@gmail.com

Abstract— In this paper, we have reviewed all the previous work done on the problem of controlling a robotic arm manipulator joint and designed a PD controller. Various techniques are being used for controlling the manipulator and the work is being done since the early 1980s. We tend to find the best possible technique for stabilizing the control system of the robotic arm joint. The purpose of this work is to find the best approach in designing a robotic manipulator that is both efficient in work and reaches the point of stability in least time possible. So, taking all precautions into account, we must design a robotic manipulator that can fulfil the purpose justly. An adaptive PD controller-based robot motion control system for a robotic arm is presented in this paper. A block diagram of the manipulator joint was used to model the system, and a closed loop transfer function was created and transformed into a state space representation. Matlab was used to plot the system's reaction against step, ramp, and parabola input. The time response of the system was calculated, and its characteristics were assessed. The peak time, rise time, and % overshoot were found to be acceptable, however the settling time was too high. Because we want the robotic arm to work as quickly as feasible, speed is a concern. So, in this paper, a PD Controller for the robotic arm was developed to reduce settling time. Kp's value was calculated to be 12 and Kd's value to be 22. Due to the PD controller's use of these values, the settling time was decreased from 15.6 seconds to 2.9 seconds, resulting in a quicker system with acceptable overshoot.

Keywords: robotic arm, PID control, Joint manipulator.

NOMENCLATURE

DC	Direct Current
AC	Alternating Current
EFJR	Electrical Flexible-Joint Robots
PID	Proportional-Integral-Derivative
ILC	Iterative Learning Control
HCI	Human-Computer Interface
MC	Modbus Communications
MIMO	Multiple Input Multiple Output
NNAX	Neural Network with Adaptive x-values
PSO	Particle Swarm Optimization
ANN	Adaptive Neural Net
PAM	Pneumatic Artificial Muscles

I. Introduction *(Literature review)*

The robotic arm is a design constituted of DC or AC motors that control the joints. Yogesh V. writes in his paper that gain margin and phase margin are very specific parameters that can be used to enhance the stability of the Robotic Arm Manipulator Joint [1]. At first, the Tan et al. approach is used to formulate the tuning measure of the system. DC motor is connected to the arm in the precision modular servo system set up and a stability boundary locus approach is used to design the PI controller. It is concluded from the formulae that the higher the gain and phase margin, the greater the stability. In designing a DC motor-based system the closed-loop response of the system with unity feedback turns out to be unstable. Hence, Tan's approach of stability boundary locus is used for designing PI tuning parameters, which concludes that the robotic arm is stabilized with improved gain margin and phase margin.

Dynamic Model of Manipulator:

This paper [2] discusses the analytical and dynamic modeling of a 3-DOF anthropomorphic robot manipulator with revolute joints. The author highlights the importance of an accurate dynamic model for control algorithm analysis and synthesis. Two modeling approaches, the Newton-Euler and Euler-Lagrange formalisms, are compared, with the latter deemed more compact and direct. The author simplifies the model by considering the center of gravity for each link, eliminating orientation changes. Kinematics are then explored, deriving position vectors in joint frames and the common coordinate system. The dynamic model is derived using the Euler-Lagrange formulation, resulting in a system of second-order differential equations. The model includes generalized coordinates, driving forces, inertia matrix, damping coefficients, Coriolis and centrifugal forces, and gravitational forces. The paper concludes by presenting a MATLAB-SIMULINK model of the 3-DOF robot manipulator dynamics, showcasing the three-link structure and input/output signals for each link.

Components of Robotic Arm Manipulator

The mechanical gripper consists of two acrylic jaws controlled by a mini servo motor for secure object gripping. The base provides support and incorporates a bearing for smooth rotational motion. Three servo motors, securely bolted to the base plate, enable precise angular rotations and position feedback. The controller converts servo signals into analog parameters, facilitating programming and synchronization of multiple servos. Male-to-male connectors establish electrical connections between components. Mechanical links, made of lightweight materials, transmit motion from servo motors to the gripper efficiently. These components collectively enable the described robotic arm to grip, hold, and transfer objects effectively. [3]

Robots (EFJRs):

The first article [4] presents a PID-controlled EFJR arm with a link positioning approach. Another article [5] evaluates the performance of five digital controllers for compensating a real robot arm joint. The controllers have been simulated in MATLAB, and the design strategies have been investigated using both discrete z-domain time methods and warped s-domain or w-plane time frames.

Computer programmed approach: Article [6] describes a computer programmed approach that uses a human-computer interface (HCI) to automate motion control in industries where human appearance is at risk. The approach includes an auto-tuning controller that can adapt to variable control. Additionally, a multivariable model with coupling terms is utilized for increased efficiency.

Model-free controller:

The literature review [7] describes a model-free tracking controller that achieves significant control by varying the gain. Prescribed performance theory is used to build robust state feedback controllers for various nonlinear systems. The recommended control method's effectiveness is demonstrated in a small film included in the report.

Double loop cascade controller:

This literature review [8] proposes a double loop cascade control for a 2-DOF controller in a single link flexible arm for trajectory tracking. The controller is effective and compared to other feedback linearization systems using non-linear mono mass modeling for controller design [9].

Adaptive controllers:

This review examines different methods to control pressure in robotic manipulators. Neural networks are utilized in several approaches, and [10] is cited as a reference for the robust adaptive control structure. These methods improve accuracy, robustness, and correct for uncertainties and disturbances [11].

IT2FP-PID (Fuzzy) controller:

An IT2FP-PID [12] controller optimized with a hybrid technique is proposed for trajectory tracking tasks and compared to traditional PID controllers. The authors conclude that these techniques improve performance and robustness.

Industrial use of robotic manipulator: This review discusses the use of virtual prototyping in the development of new car components. The authors developed a control system for testing automatic transmis sion systems using a robot manipulator [13][14]. The MC standard is widely used, but commercial applications typically only require certain building blocks.

Input torque limit compensator:
A solution for generating a robot arm route with the necessary shape and input torque limit to regulate minimum synchronization is proposed. The proposed algorithm takes into consideration the manipulation dynamics and employs somewhat conservative torque constraints. The technique can handle most actuators encountered in reality and can be used to compare different trajectory planning methods. [15-16].

Mathematical modelling approaches:
A mathematical framework based on Lagrangian dynamics for controlling linear and rotary springs in flexible joint robotics is presented. The authors propose an adaptive approach that accounts for joint elasticity and successfully controls general location adaptation. An adaptive control of a flexible joint controller extending the adaptive algorithm of a rigid robot was developed. [17]

Compensator for robotic controller:
The adaptive force/position control of flexible articulated robots and factors that affect their performance are discussed. Appropriate adaptive control techniques and adaptive non-saturation limiters have been designed to address the challenges of dynamical instability and actuator saturation. A new pro-compensator to avoid the failure of the attenuator during design and eliminate adaptative non-saturating singularity is suggested. [18].

Lyapunov technique for PID
A control method for closed-loop systems that utilizes an enhanced EHGO to reduce ultimate error limits is examined. The method combines continuous PID simulations with an original controller to improve transient response performance while maintaining accurate monitoring and estimation. The suggested strategy is confirmed by numerical estimation on the PUMA560 and is compared favorably to other popular approaches. [19].

EHGO type controllers:
The use of closed-loop systems in EHGO for enhanced transient performance without compromising tracking accuracy is discussed. [20] An alternate upper limb training strategy with robotic assistance for unattended stroke therapy is presented. The suggested approach allows patients to receive unsupervised therapy and training at home. The performance of the PID system can be improved by changing the proportional gain and the gain value of the controller.

Table:

Paper	Approach	Comments
PI controller design for one joint robotic arm	Gain and phase margin tuning rules have been created for PI	.The suggested method is founded on the stability boundary locus.
Multi-input multi-output adaptive torque control of 9-DOF hyper-redundant robotic arm	A Multi-input multi-output (MIMO) is used for advanced robotic arm output sensing	MIMO proposes better torque control output
Robotic Manipulator Control Using PD-type Fuzzy Iterative Learning Control	PD-type Fuzzy ILC is used for the 2DOF robotic arm manipulator	High stability convergence
Adaptive linear controller for robotic manipulators	In this approach an adaptative linear controller is used for robotic arm	Controller directs each manipulator joint's output to follow a predetermined trajectory at specific points.
Input-state feedback linearization control of a single-link flexible robot arm moving under gravity and joint friction	Mitsubishi PA-10 robot arm is used as an experiment of input state feedback linearization control	Controller can track very fast trajectories with required transient and steady-state performance
Modeling, observation, and control of hysteresis torsion in elastic robot joints	a 2-DOF controller is in charge of maintaining the joint position while dealing with Coulomb friction disturbances, and in its outer loop, an input-state	approach outperforms the competition in terms of settling time, maximum overshoot, and residual vibrations

	feedback linearization	
Compliance Control for Robot Manipulation in Contact with a Varied Environment Based on a New Joint Torque Controller	An ADRC and DCRA approach on torque controller is used.	The methods used by the controller to change parameters are straightforward and have been proven in practical applications.
Interaction control of robotic manipulators without force measurement	This controller is then optimized by altering various parameters, such as antecedent MFs, to carry out trajectory tracking tasks	Efficiency of the suggested controller is verified using a thorough robustness study in the presence of diverse nonlinear dynamics
Control system design of robotic manipulator for testing of shifting system	This block covers the improvement of the transferring device version and manage algorithms, hardware-in-the-loop	Simulink environment's RexLib bundle makes it feasible
A framework of adaptive fuzzy control and optimization for nonlinear systems with output constraints	special technique is given which appoint adaptive NNs to account for the dynamic manipulate robot manipulator machine	The time-various disturbance changed into more or less modelled the use of virtual outputs, and the unknown dynamic version of the robot manipulator changed into anticipated the use of NNs.
Robust adaptive control of a bio-inspired robot manipulator using bat algorithm	to generate a route with the necessary shape and input torque limit to regulate the minimum synchronization of a mechanical robotic arm	The best course of action may violate the permissible region's limit, as was already said, creating a scenario that is fairly perilous
Modeling, observation, and control of hysteresis torsion in elastic robot joints	sliding mode control adaptable and unaltered control with adaptive neural	The outcomes demonstrate that the fit affects the selected control approach

	net ANN control are developed	
28 Predefined performance adaptive control of robotic manipulators with dynamic uncertainties and input saturation constraints	A closed loop system's ultimate error limit can be reduced by a design parameter which is a quick and efficient way to tune a dynamic parameter	the Lyapunov technique and singular control theory respectively show that the subsystem and closed loop control system are stable
30 Robotic arm for unsupervised stroke rehabilitation: A pilot study using PID controller	Closed loop systems' transient performance is enhanced by dynamic process parameters in EHGO without compromising tracking	By changing the intensity of the control schemes in the PID system performance may be enhanced S approach to the set point the gain value of the controller might be raised

Table 1: Table of approach

II. Methodology

In this paper, the implementation of a modelling and control system for robotic hands is presented. The telemanipulation system's motion control is discussed. The hardware and software utilized in the suggested work are first described in the following sections. The robotic manipulator is a nonlinear system having coupled effects among each joint or translational variable since it is a complicated multi-body dynamic system. Accurate dynamic equations, like the one employed by Low, 2013 [21], are a key component of many control techniques for robotic manipulators. Following that, the modelling procedure, the design of the control scheme, the simulation, and the experimental findings for a single joint are provided. The system's experimental investigation for built-in telemanipulation. The system's components are described, and the governing equations are modelled, as the initial stage. According to [1] the main actuator that is most of the mechatronics systems is PMDC motor. In case of the arm manipulator, PMDC motor is joined with the joint of arm, whereas the arm joint is designed as potentiometer. Using the Kirchhoff's Law and energy balance equations, we were able to build the transfer function of the joint as done. An angular position sensor is dedicated which gives closed loop transfer function. System modelling in State space can be a better tool for simplifying the equations which can be used to obtain output in software, as in [22]. The next step of our approach will be testing the system for stability. The software used for this purpose is MATLAB and Simulink. In [23], kinematic modeling of robotic arm manipulator is done using MATLAB. We'll plot the root locus diagram for this purpose. The roots of the system's characteristic equation (the Laplacian) are displayed as a function of the control variables in root locus plots. It is feasible to assess the stability of various control variable values by looking at these graphs. With the development of open and closed loop characteristics, we can describe Kp for the system. Various researches as in [12-15] use other controller types such as fuzzy logic system, haptic system, neural based network etc. but we are constrained to use Proportional Integral controller unit in our problem. Therefore, the next step is to develop the equations for Ti. The approach we are using is simple and easier to develop for the purpose of designing a 2DOF robotic arm manipulator. [24]. Fig. 1 depicts a simplified equivalent representation of the two components of an armature-controlled PMDC motor.

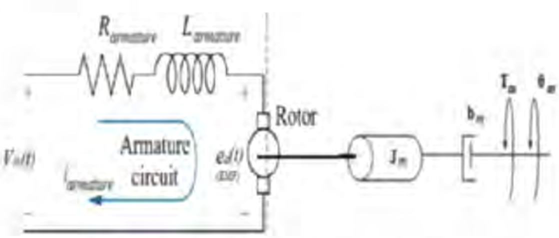

Figure 1: PMDC motor (Ebrahimi,2019)

III. Mathematical Modelling

The block diagram of the system is given as

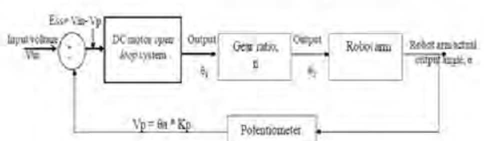

Figure 2: Block diagram (Ebrahimi, 2019)

Now we find the governing equations for the system to generate transfer function. As a continuation of Fig (1), the system can be represented as:

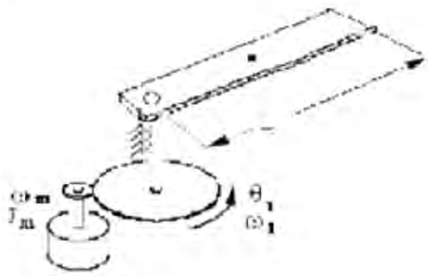

Figure 3: Single joint robot arm (Ebrahimi, 2019)

The motor torque is given by Eq (1). The generated EMF voltage, ea, is given by Eq (2).

$$Tm = K_t i_a \quad (1)$$

$$e_a = K_b \omega_m = K_b \frac{d\theta_m}{dt} \quad (2)$$

Applying Kirchhoff's law around the electrical loop, substituting, result in Eq (3). Taking Laplace transform and rearranging and the result is stated in Eq (4):

$$L_a \frac{di}{dt} + R_a i = V - K_e \frac{d\theta_m}{dt} \quad (3)$$

$$I_a(s) = \frac{V(S) - K_e S\theta_m(s)}{R_a + L_a S} \quad (4)$$

Performing the energy balance process for equations; the sum of the torques must be equal to zero, which yields Eq.(5), Taking Laplace transform and rearranging, result is stated in Eq(6):

$$K_t * i - T_{Load} - J_m\left(\frac{d^2\theta}{dt^2}\right) - b_m\left(\frac{d\theta}{dt}\right) = 0 \quad (5)$$

$$K_t I(s) = (J_m s + b_m) s\theta(s) \quad (6)$$

Putting Eq. (4) in Eq. (6) and rearranging, which yields the transfer function given by Eq. (7) in terms of output motor shaft angle θ□ and the input voltage V(s).

$$G_m = \frac{\theta_m(s)}{V(s)} = \frac{K_t}{s[(R_a + L_m s)(J_a s + b_m) K_b + K_t]} \quad (7)$$

The total equivalent inertia, Jeq and total equivalent damping, beq at the armature of the motor are given by:

$$b_{eq} = b_m + \frac{b_{load}}{n^2}, \quad J_{eq} = J_m + \frac{J_{load}}{n^2}$$

By substituting J_{eq} and b_{eq} in E_q. (7), the total equivalent transfer function with respect to input voltage V_{in} and the Arm-load output angular positionθ_{load}, is stated in Eq. (9). The gear system has the transfer function (gear ratio n), is included in this transfer function.

$$G(s) = \frac{\theta_{load}(s)}{V_{in}(s)} \quad (8)$$

$$G(s) = \frac{K_t \times n}{L_a J_{eq} s^3 + (R_a J_{eq} + b_{eq} L_a) s^2 + (R_a b_{eq} + K_t K_b) s}$$

(9)

The nominal values for the robotic arm manipulator that is to be designed;

arm mass	M = 8 Kg
arm length	L=0.4 m
Viscous damping constant	b = 0.09 N.sec/m

Table 2: Values for system parameters

The following are the nominal values for the parameters used in electric motor:

B_{eq}	0.119971;
J_{eq}	0.012665217;
K_t	0.023 N-m/A;
K_b	0.023 V-s/rad;
R_a	1 Ohm;
L_a	0.23 Henry;

Table 3: Values for system parameters

For simplicity, n=1.

Substituting the nominal values of parameters into transfer function gives open loop transfer function.

Eq. (9):

$$G(s) = \frac{0.023}{0.02913\, s^3 + 0.1543 s^2 + 0.1205 s}$$

For closed loop transfer function T(s):

$$\frac{C}{R} = T(s) = \frac{G}{1 + G(s)}$$

Solving for T(s) gives closed loop transfer function as:

$$T(s) = \frac{0.023}{0.02913\ s^3 + 0.1543\ s^2 + 0.1205\ s + 0.023}$$

Modelling in time Domain

Converting transfer function to time domain using state space modelling in MATLAB

State space:

$$X = \begin{bmatrix} -5.2969 & -4.1366 & 0 \\ 1 & 0 & 0 \\ 0 & 1 & 0 \end{bmatrix} X + \begin{bmatrix} 1 \\ 0 \\ 0 \end{bmatrix} U \quad (10)$$

$$Y = [0 \quad 0 \quad 0.7896\ ] X + [0]$$

IV. Implementation

Using the closed and open loop transfer function of the system, we tend to find system characteristics and response. For obtaining responses against various inputs, we opted for MATLAB as it was convenient and easily applicable.

A. Time Response of our system for step input

Using transfer function, for step input:

$$C(s) = \frac{0.023}{s(0.02913\ s^3 + 0.1543\ s^2 + 0.1205\ S + 0.023)}$$

$$C(s) = \frac{0.023}{s(s + 0.298488\ )(s + 0.601917)(\ s + 4.39465)}$$

Taking partial fractions

$$C(s) = \frac{0.2913}{s} - \frac{0.0619964}{s + 028488} + \frac{0.0332033}{s + 0.64197} + \frac{0.000336879}{s + 4.39465}$$

Taking inverse Laplace.

$$C(t) = 0.02913 - 0.0619964\ e^{-0.2985} + 0.0332\ e^{-4.39465} - 0.000337\ e^{-4.39465}$$

Where 0.02913 is forced and $-0.0619964\ e^{-0.2985} + 0.0332\, e^{-4.39465} - 0.000337\ e^{-4.39465}$ is natural response.

B. System Characteristics

We use MATLAB to obtain system characteristics

```
    RiseTime: 8.6776
SettlingTime: 15.6184
 SettlingMin: 0.9029
 SettlingMax: 0.9991
   Overshoot: 0
  Undershoot: 0
        Peak: 0.9991
    PeakTime: 25.8854
```

Figure 4: MATLAB output

We must first reduce the system to find the damping ratioζ, settling timeT_s, ω_n.

$$T(s) = \frac{0.023}{(s+4.39465)(\ s+0.29862)(\ s+60132)} \quad (10)$$

$$T(s) = \frac{0.023}{(s+4.4)(\ s^2+0.9\,s+0.1804)} \quad (11)$$

Natural frequency:

$$\omega_n^2 = 0.1809$$
$$\omega_n = \ 0.42474$$

Damping ratio:

$$2\zeta\omega_n = \ 0.9$$
$$\zeta = 1.05$$

Since the three of poles are x-axis so the system is critically damped. The responses are given below

Step response:

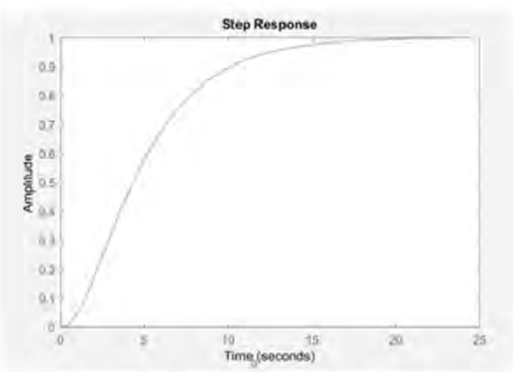

Figure 5: Response plot of Step input

Ramp response:

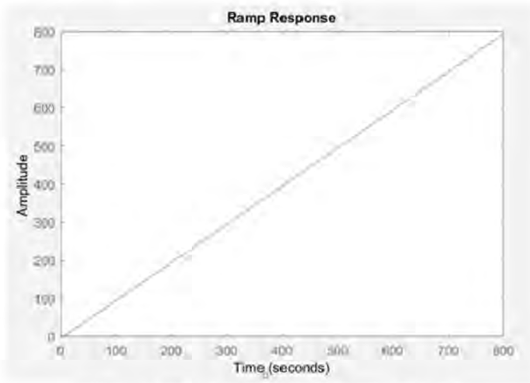

Figure 6: Response plot of Ramp input

Parabolic response:

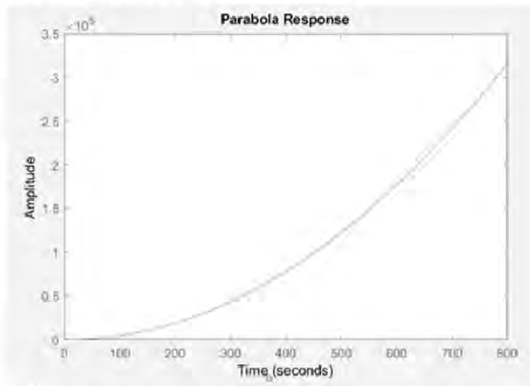

Figure 7: Response plot of Parabolic input

C. Stability of System

Transfer function:

$$T(s) = \frac{0.023}{0.02913\,S^3 + 0.1543S^2 + 0.1205S + 0.023}$$

(11)

Poles are

$$s_{1,2,3} = -0.2985, 0.601917, -4.39465$$

(12)

So, the transfer function has poles in left half plane only, so it is a stable system.

Gain limits:

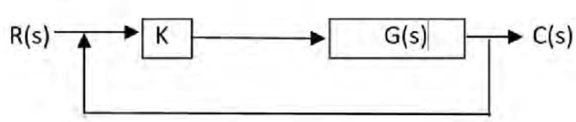

Figure 8: Block diagram with P-controller

$$T(s) = \frac{0.023K}{0.02913\,S^3 + 0.1543S^2 + 0.1205S + 0.023K}$$

With the help of Routh Hurwitz technique, we can find the whether the system is stable or not and for which value of it is stable. Making Routh Hurwitz Table:

s^3	0.02913	0.1205
s^2	0.154245	0.023K
s^1	$\frac{-\begin{vmatrix} 0.02913 & 0.1205 \\ 0.154245 & 0.023K \end{vmatrix}}{0.154245}$	0
s^0	$0.023k$	0

Table 4 Routh Hurwitz Table

- For the system to be stable:

$$\frac{0.018586523 - 0.0006699K}{0.154245} > 0$$

$0 < k < 27.745$

- For the system to be marginally stable:
  $k = 27.745$
- For the system to be unstable:
  $k > 27.745$

Since in the beginning we made assumption that K>0 therefore our P-controller gain K varies from 0 to $+\infty$ or $k > 0$.

D. Steady State Errors

For the steady state error:

$$G(s) = \frac{0.023}{0.02913\,s^3 + 0.1543s^2 + 0.1205s}$$

$$G(s) = \frac{0.023}{s(0.02913\,s^2 + 0.1543s + 0.1205)}$$

For step, ramp and parabolic inputs:

$$e(\infty) = e_{step}(\infty) = \frac{1}{1+k_p} = \frac{1}{1+\lim_{s\to 0} G(s)} = \frac{1}{1+\infty} = 0$$

$$e(\infty) = e_{ramp} = \frac{1}{\lim_{s\to 0} s\,G(s)} = \frac{\frac{1}{0.023}}{0.1205} = 5.24$$

$$e(\infty) = e_{parabola}(\infty) = \frac{1}{1+\lim_{s\to 0} s^2 G(s)} = \frac{1}{0} = \infty$$

Therefore, the system is type 1

E. Plotting root locus:

Plotting root locus using MATLAB command rlocus:

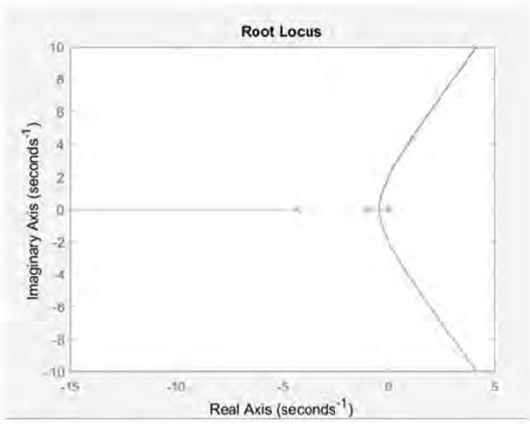

Figure 9: Root locus plot

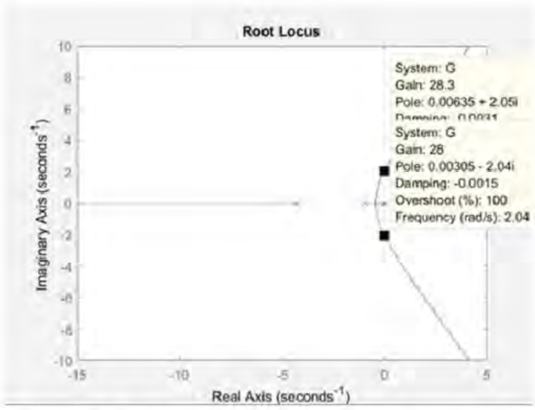

Figure 10: Root locus plot with system Characteristics

v. Controller Design:

By plotting the response of the system against step input, it is observed that steady state error is 0 and for ramp input error is 5.24 and for parabolic input the errors appear to be infinity because the system is type 1 system and, in that case, k_a is 0 making the error infinity. Moreover, a settling time of 15.6 sec is observed, which is not desirable under the situation and is meant to be improved. Since the required characteristics of robotic arm is max 3 sec settling time and a maximum of 6% over-shoot. Less settling time and faster response along with least possible steady-state error was the requirement of the situation. Since the system response is ''Critically Damped'' corresponding to ζ=1.0 . So the only issue with the system appears to be settling time. Settling time was tried to be improved by usage of only P-controller but the results were not satisfying as the system starts oscillating. The best approach to the solution was design of PD-controller to cater settling time and over-shoot at the same time. The usage of PD-controller proved to be useful and gave the response that was required, the settling time was reduced from 15.6 sec to 2.9 sec and the over-shoot was 5.8% which is allowable in our system. By using PID controller the settling time can be improved about 0.5sec more than PD but 0.5sec is not a much difference to shift from PD to PID controller as we need to keep the things as simple as we can so, we used PD-Controller for our system. MATLAB PID-Tuner was used to find the required values for gains of P and D controllers and then the values of k_p and k_d were altered until the required response was achieved. The improved system response is as follows:

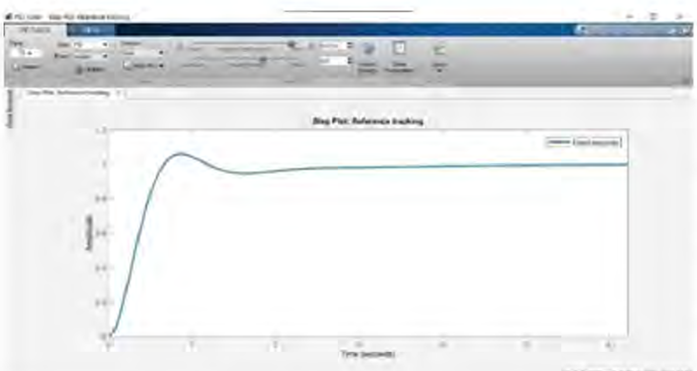

Figure 11: Tuned response plot of the system

Controller Parameters

	Tuned
Kp	12.8711
Ki	n/a
Kd	22.5272
Tf	n/a

Performance and Robustness

	Tuned
Rise time	0.438 seconds
Settling time	2.92 seconds
Overshoot	5.87 %
Peak	1.06
Gain margin	Inf dB @ Inf rad/s
Phase margin	60 deg @ 3.21 rad/s
Closed-loop stability	Stable

Figure 12: Tuned system characteristics with PD-Controller

V. Conclusion:

Robotic arms are generally used in industry to carry out a specific task quickly and accurately, These Robots usually use motor to drive them and consist of arm and joints. So, this study presents an adaptive PD controller-based robot motion control system. A suggested approach for calculating the arm joints' angles along any path. So, we have modelled our system using block diagram of manipulator joint. Closed loop transfer function was formed using block diagram and then the transfer function was converted into state space representation. Time response was calculated to check the force response and natural response. System characteristics were calculated and our system's settling time was too large but others thing like peak time, rise time, percentage overshoot were all OK and then we checked the stability of our system and our system came out to be stable having all the poles on left half plane and then unit Step response was plot and the system was following the input accurately but the settling time was way much greater than the desired settling time. There was zero error in step input showing that our system has zero error in position. There was 5 percent error in ramp input and infinity in parabola input that shows that our system is type 1 system so we can also control velocity of our system. As we want the robotic arm to be as fast as possible so it can work faster. So for the reduction of settling time PD Controller is designed in this paper for the robotic arm. The value of Kp came out to be 12 and the value of Kd came out to be 22. So, by using PD controller having these values, the controller reduced the settling time from 15.6 sec to 2.9 sec the peak time was also reduced and the rise time was also reduced but the overshoot was 5.6% which is acceptable in our case of robotic arm so by reducing the settling time the system becomes faster as the robotic arm approaches the input in 3 sec so, it's quite a good system.

A. COMPARISON OF IMPROVED AND UN-IMPROVED SYSTEM RESPONSES:

	Un-improved	Improved
Steady-state error	0	0
Settling time	15.6184 seconds	2.9 seconds
Overshoot	0 %	5.8 %
Rise time	8.6776 seconds	0.438 seconds
Peak time	25.8854	1.06

Table 5 Comparison Table

References

[1] Hote, Y. V. (2016). PI controller design for one joint robotic arm. 2016 14th International Conference on Control, Automation, Robotics and Vision (ICARCV), 1–6..

[2] Kardoš, J. "The simplified dynamic model of a robot manipulator." Proceedings of the 18th International Conference. 2010.

[3] Pawar, Vaibhav, et al. "Review on design and development of robotic arm generation-1." Int J Innov Sci Res Technol 3.3 (2018).

[4] Izadbakhsh, Alireza, and Saeed Khorashadizadeh. "Single-loop PID controller design for electrical flexible-joint robots." Journal of the Brazilian Society of Mechanical Sciences and Engineering 42.2 (2020): 91.

[5] Piltan, Farzin, et al. "PUMA-560 robot manipulator position computed torque control methods using Matlab/Simulink and their integration into graduate nonlinear control and Matlab courses." International Journal of Robotics and Automation 3.3 (2012): 167-191.

[6] Shin, Sungtae, Reza Tafreshi, and Reza Langari. "EMG and IMU based real-time HCI using dynamic hand gestures for a multiple-DoF robot arm." Journal of Intelligent & Fuzzy Systems 35.1 (2018): 861-876.

[7] Abouaïssa, Hassane, and Samira Chouraqui. "On the control of robot manipulator: A model-free approach." Journal of Computational Science 31 (2019): 6-16.

[8] Jiang, Naijing, et al. "Cascade control of underactuated manipulator based on reinforcement learning framework." Proceed ings of the Institution of Mechanical Engineers, Part I: Journal of Systems and Control Engineering 237.2 (2023): 231-243.

[9] Piltan, Farzin, et al. "Design novel fuzzy robust feedback linearization control with application to robot manipulator." International Journal of Intelligent Systems and Applications 5.5 (2013): 1-10.

[10] Elsisi, Mahmoud, et al. "An improved neural network algorithm to efficiently track various trajectories of robot manipulator arms." Ieee Access 9 (2021): 11911-11920.

[11] Hsia, T. "Adaptive control of robot manipulators-a review." Proceedings. 1986 IEEE International Conference on Robotics and Automation. Vol. 3. IEEE, 1986.

[12] Gaidhane, Prashant J., et al. "Design of interval type-2 fuzzy precompensated PID controller applied to two-DOF robotic manipulator with variable payload." ISA transactions 89 (2019): 169-185.

[13] Ali, Md Hazrat, et al. "Vision-based robot manipulator for industrial applications." Procedia computer science 133 (2018): 205-212.

[14] Kaltsoukalas, K., S. Makris, and G. Chryssolouris. "On generating the motion of industrial robot manipulators." Robotics and Computer-Integrated Manufacturing 32 (2015): 65-71.

[15] Alvarez-Ramirez, Jose, Victor Santibanez, and Ricardo Campa. "Stability of robot manipulators under saturated PID compensation." IEEE Transactions on Control Systems Technology 16.6 (2008): 1333-1341.

[16] Canudas de Wit, C., et al. "Adaptive friction compensation in robot manipulators: Low velocities." The International journal of robotics research 10.3 (1991): 189-199.

[17] Wang, Jun, Qingni Hu, and Danchi Jiang. "A Lagrangian network for kinematic control of redundant robot manipulators." IEEE Transactions on Neural Networks 10.5 (1999): 1123-1132.

[18] Yoo, Byung Kook, and Woon Chul Ham. "Adaptive control of robot manipulator using fuzzy compensator." IEEE Transactions on fuzzy systems 8.2 (2000): 186-199.

[19] Rocco, Paolo. "Stability of PID control for industrial robot arms." IEEE transactions on robotics and automation 12.4 (1996): 606-614.

[20] Zhang, Xinyu, et al. "Continuous PID-SMC based on improved EHGO for robot manipulators with limited state measurements." Journal of the Franklin Institute 357.15 (2020): 10648-10668..

[21] K. H. LOW, HENG WANG, KIM MEOW LIEW, YIYU CAI. "MODELING AND MOTION CONTROL OF ROBOTIC HAND FOR TELEMANIPULATION APPLICATION", International Journal of Software Engineering and Knowledge Engineering, 2011

[22] Serrezuela, R. R., Chavarro, A. F. C., Cardozo, M. A. T., Toquica, A. L., & Martinez, L. F. O. (2017). Kinematic modelling of a robotic arm manipulator using Matlab. ARPN Journal of Engineering and Applied Sciences, 12(7), 2037-2045

[23] Koditschek, D. (1984). Natural motion for robot arms. The 23rd IEEE Conference on Decision and Control. doi:10.1109/cdc.1984.272106

[24] Ebrahimi, N. (2019). Modeling, simulation and control of a robotic arm. In engrXiv. https://doi.org/10.31224/osf.io/t8fsr

Adaptive routing protocol for Industrial Wireless Network

Bilal Muhammad Khan
Department of Electrical Engineering, National University of Sciences and Technology, NUST, Islamabad
bmkhan@pnec.nust.edu.pk

Abstract—In Mobile Ad-Hoc Networks discovering and maintaining link between the nodes is difficult. Mobility of nodes in MANETs provides a challenging problem for designing an efficient and reliable routing strategy for data transmission. Most of the routing protocol uses control signalling to determine the active link in the network. The duration of these signals affects the network performance like throughput, reliability and energy. This paper provides simulation analysis to find optimize values for the control signals. To the best of author knowledge this adaptive approach is first of its kind and produces enhanced results with less complexity. The paper proposes a novel protocol namely Adaptive AODV (AAODV) for the selection of control signals according to network parameter and topology for optimum results. The result shows increase in throughput of AAODV by 28% with maintaining high reliability as of Conventional AODV.

Key words
Adaptive, AODV, control signals, mobility

Introduction

In networking, the infrastructure based networks requires a centralized point for communication where tracking path is difficult for wireless network. These networks are now being replaced by infrastructure-less networks, called as ad-hoc network, which are self-configuring multi-hop network for mobile nodes. Each node in ad-hoc network communicates directly with other nodes or by using a multi-hop utility.

In Mobile Ad-hoc Networks (MANETs), link between the nodes makes and breaks frequently [2]. Each node in mobile network needs updated information of its surrounding/local neighbours to maintain and discover new links. Several reactive and proactive routing protocols have been proposed for ad-hoc network [8] which includes Optimise link state routing protocol (OLSR), Adhoc on Demand Distance vector Routing (AODV), Destination sequenced distance vector (DSDV), Wireless routing protocol (WRP), Dynamic source routing (DSR), Associative base routing (ABR). These protocols use different techniques for route discovery and link management [6], [5]. The one common technique for Link Connectivity Management (LCM) is the use of control signals.

The control signal is broadcast in a network by a node periodically to determine active links. Each node updates its table depending on the response it gets after sending this signal. The frequency of such intervals plays an important role in network efficiency. A very high frequency can bring interference and wastes bandwidth [7] whereas low frequency will cost a delay in determining link failure.

Section I gives related work, section II gives the description of AODV protocol. Section III includes control signal and its effects, Adaptive AODV analysis and theory is explained in section IV, simulation and results in section V and conclusion in section VI.

I. Related work

Various adaptive routing protocols have been presented using different routing and LCM techniques for high quality ad-hoc network.

In [5] it is shown that the network performance can be enhanced by using hello messages. PDR and energy consumption gets better with the use hello messages in AODV routing protocol for ad-hoc network.

The factors influence the utility of hello messages is discussed in [4], with static and mobile node under different environment. They found that allowed hello message loss settings, discrepancy between data and hello message size and 802.11b packet handling can affect the network efficiency which can vary with network topology, node speed and surrounding environment.

The choice of MAC and physical layer also affect the hello parameter for ad-hoc network [6]. The effect of these realistic layers on self-organizing protocol is described in [6].

Frequency of hello messages also has its impact on network efficiency. The relationship between the transmission frequency of the hello messages and the sensing timer expiration value with the network node's mobility is presented in [1]. They find out the probability of link existence during hello message interval and use it with timer expiration to determine the link failure.

In order to reduce the overhead and quick link detection, Adaptive Hello messages (AH) is introduced in [2]. AH is designed for highly dynamic network where hello interval varies according to actual situation of nodes.

Fuzzy algorithm designed for adaptive optimization of hello messages in wireless ad-hoc network is presented in [7]. The fuzzy criterion is based on node's transmitting power and its speed. They design a set of rules for fuzzy algorithm which adopt hello interval according to those rules and gives optimize result. Using fuzzy logic network configuring parameter can be determined more accurately than the static values.

A cognitive routing approach to improve efficiency and reliability of AODV is presented in [11]. In this paper "First Fast Second Reliable" principle is introduced to produce an adaptive AODV by discovering the shortest and most reliable route for transmission.

II.AODV

AODV is a reactive routing protocol which discovers routes for communication on-demand. The performance of AODV has found optimum for ad-hoc networks. The results in [8], [9] shown AODV has less overhead better throughput and eliminates few problems existing in other routing protocols. It determines route by broadcasting 'Route Request (RREQ)' message in a network [9], [10]. The protocol makes sure that discovered routes do not contain loops and it tries to find the shortest route possible. AODV is also able to handle changes in routes by forwarding Route ERR or (RERR) [9] [10] and can create new routes if there is an error or stale route present in a network.

III. Control Signal

Control Signals are used in several routing protocol for maintaining links between nodes in an ad-hoc network. A node in a network broadcast a "HELLO MESSAGE" as a control Signal to update its routing table. Hello message comprises of two factors, Hello Interval and Allowed Hello Loss [4]. These parameters have great impact on network performance which can vary with nodes mobility [1], [2], [5] and network topology. The frequency and interval duration of this Control Signal vary the throughput efficiency [7] and energy [7], [3] consumption of node. These control signals can be used in an effective way to enhance the network performance.

IV. Adaptive AODV

In this paper we have proposed an Adaptive AODV protocol for static and mobile nodes to enhance the efficiency of ad-hoc network. This protocol is less complex and uses little over head to provide maximum throughput and reliability with minimum energy consumption. The interval of control signals can vary the network efficiency with respect to actual situation and network parameters. For highly dynamic networks, control signal interval should make adaptive so the network efficiency can be maintained at a certain level. Throughput variation in network is considered for several data rate and node speed to make hello interval adaptive accordingly. This approach can give the optimize result for network efficiency with less complexity.

The effect of network parameters on performance metric has also shown mathematically. Throughput (Ъ) of the network is dependent on data rate (ɖ), mobility (m), rate of packet collision (þ), hello interval (Ḫ). For high data rate more data packets are being transmitted causes the throughput to increases but for very high data rate packet collision may occur which reduces the throughput. Also path breaking between nodes caused by node movement also varies the throughput efficiency which is dependent on node's mobility and hello interval which determines the delay to detect and recover the breaking link. Equation I gives the generalize equation for network throughput,

$$\text{Ђ} = \frac{\text{ḑ}}{\int \text{Ḩ}\,.m.\text{þ}} \qquad \text{(Equation I)}$$

Reliability (Ɍ) is another important factor in determining network performance. It can be define as the successful reception of transmitted data at receiver end with minimum delay and maximum accuracy. The ratio of received packet to the transmitted packets is defined as ɳ. Mathematically reliability of the network is expressed in,

$$\text{Ɍ} = \frac{\text{ɳ}}{\text{Ḩ}} \qquad \text{(Equation II)}$$

Energy (Ẽ) is one other performance parameter taken in account. The node transmitting data at high rate deplete more energy due to more packet transmission in less time. Energy consumption in node also changes with varying mobility. The node moving with high velocity requires more power for its movement. Control signalling also consumes power for transmitting and listening to hello messages. For greater hello interval more energy will be required to listen for hello message for a long duration. Equation III shows the energy consumption of network mathematically,

$$\text{Ẽ} = \int \text{Ḩ} + m + \text{ḑ} \qquad \text{(Equation III)}$$

V. Simulation and Results

Simulation has been done using MALTAB-Simulink R2012a with true-time beta 2.0 library. The network comprises of seven wireless nodes placed to an area of 30 x 30 meter. This protocol can be implemented to a scalable network. The transmitting range of each node is 0.5 meter. For mobility of nodes the mobility model used is Random Way Point (RWP) with pause time of 0.1 seconds. For conventional AODV, one static hello interval used is 1 second which has been made adaptive for AAODV. Mobility of nodes has also varied to get effective results for various speeds. Results are obtained for both static and mobile network using Adaptive AODV protocol and compare with conventional AODV. Network performance metric such as throughput, reliability and energy has been analysed for several data rate and node's speed. These results have also summarized in table 1, 2 and 3 for static, low speed and high speed nodes respectively.

a. Throughput for Static Nodes

Throughput for AODV and AAODV with static nodes is shown in Figure 1. The graph of AAODV shows up to 11% better performance compare to conventional AODV. The throughput has been examined at various data rate but efficiency of AODV with static hello interval does not exceed from Adaptive AODV. At slow data rate throughput for both protocol is almost similar because bandwidth is under-utilize and network can bear large interval for control signals. At high data rate the throughput for AODV is dropped which is maintained in AAODV by varying its control signal interval. At high rate network needs most of the time to be utilize for data transmission so AAODV reduce its control signal interval for high data rates which causes its throughput to increase. Whereas in conventional AODV the control signal interval is fixed. It does not vary its bandwidth utilization and consume fixed amount of time in link determination between the nodes which causes most of the data packets to be lost due at high transmitting rate. AAODV controls its control signal interval depending on source node data rate for static network. Distinct throughput efficiency can be observed between AAODV and AODV results using this adaptive approach.

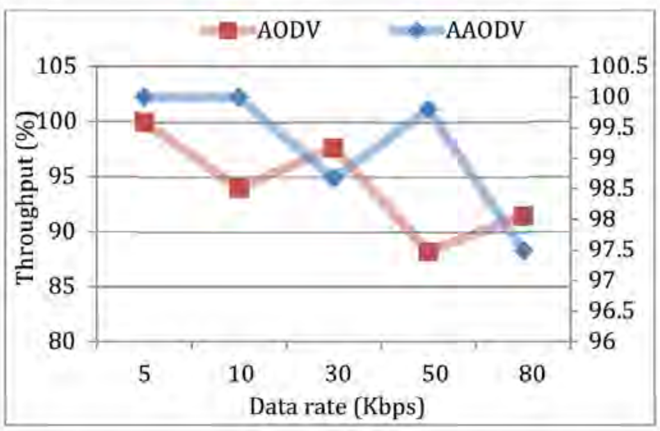

Figure 1, Throughput comparison of AAODV and AODV protocols.

b. Reliability for Static Nodes

From Figure 2, it can be observed that reliability of the static network is maintained in Adaptive AODV. Adapting control signal interval does not affect the network's reliability. The AAODV sets its interval so as to have maximum data transmission on best available active link. This approach enhances its performance by maintaining its reliability. A slight drop of about 0.1% in reliability of AAODV is observed at high data rate. This is due to the loss of control signal as a result of collision at high data rate. But this small difference is acceptable at cost of increased throughput. Hence with similar high reliability as of conventional AODV the optimize results for static network can be obtain by using AAODV.

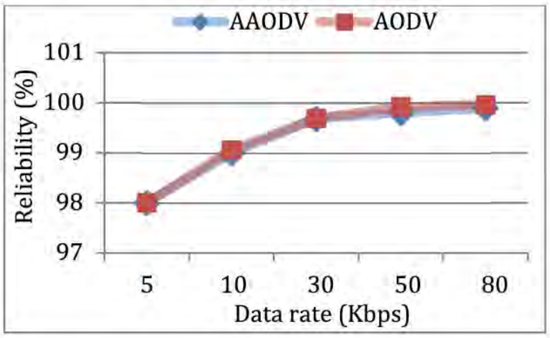

Figure 2, Reliability comparison of AAODV and AODV protocols.

c. Energy for Static Nodes

Figure 3 shows the energy consumption of AODV and AAODV. It is visible from graph that AAODV does not consume any extra energy for using adaptive control signal interval. When the data rate is low the hello interval value in AAODV is set large enough to keep the link knowledge updated with maximum throughput. This greater Interval value consumes same level of energy for both AODV and AAODV; However as data rate increases AAODV reduces control signal interval which reduces the energy consumed by control signal but at the same time more data transmission requires more energy. This keeps the energy consumption of the both protocols approximately at same level but enhances the network's performance of AAODV by transmitting more data. AODV consume more energy for control signals even at high data rate which drops its efficiency. Whereas AAODV uses the same power and provide enhanced performance by making energy consumption indirectly adaptive among data transmission and hello interval. So introducing adaptive approach to AODV do not cost any additional energy overhead and perform better than AODV under same power utilization.

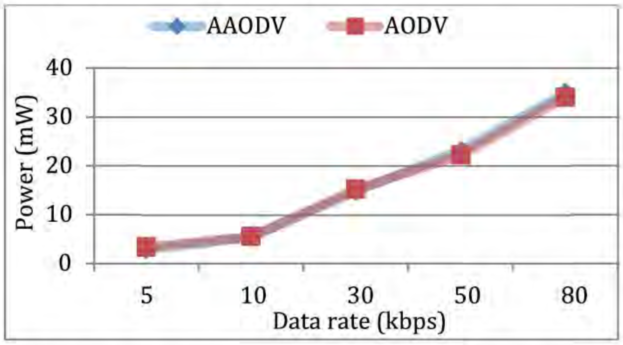

Figure 3, Energy comparison of AAODV and AODV protocols.

d. Throughput for Slow Mobile Nodes - Speed 4m/s

Throughput for mobility is simulated for two different node speeds. Results for slow mobility of 4m/s are shown in Figure 4, where it can observe that AAODV also perform better in mobile scenario. In mobile networks the control signal interval is made adaptive on the basis of data rate and nodes mobility. When the mobility is high the Adaptive AODV reduces its interval to get maximum updated link information but at the same time it also considers the data rate so that the selected interval should not lower the efficiency. This adaptive approach for controlling interval duration provides an optimize result with greater efficiency in comparison with conventional AODV. The performance of AAODV for speed of 4 m/s is up to 16% better than conventional AODV. This degraded performance of AODV because of its static control signal interval. Due to large value of control signal interval the node's routing table contains some of the false route. These false information causes the data packets transmitted on those routes to be lost which reduces the efficiency of conventional AODV. In comparison the Adaptive AODV controls its control signal interval with data rate and mobility. With increase in data rate the Adaptive AODV sets an optimum value for interval to get the maximum throughput with given node mobility. This varying control signal interval keeps the node table updated which reduces the data loss in the network. Hence AAODV increases the throughput for various data rate with mobile nodes. The result shows that the performance of AAODV is more effective with increased data rate in mobile network.

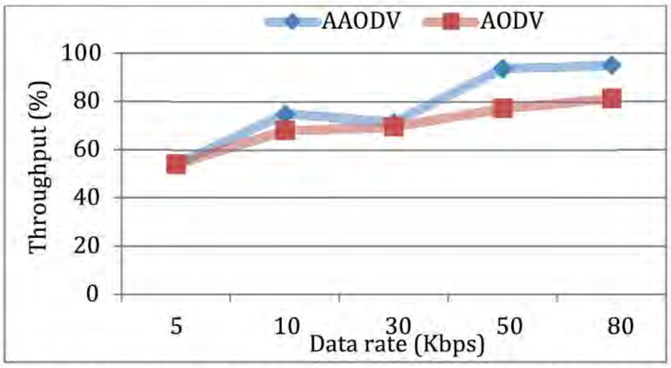

Figure 4, Throughput comparison of AAODV and AODV protocols with slow mobility - Speed 4m/s

e. Reliability for Slow Mobile Nodes - Speed 4m/s

Reliability for slow speed nodes of 4m/s is shown in figure 5. The optimization in Adaptive AODV for mobile network does not affect the network reliability and it is maintained at the same level as of AODV for low data rate. However very small change in reliability is observed for high data rate. This is because the AAODV aims to provide maximum throughput along with reliable communication; Hence the value of control signal interval is so selected that it keeps the list of current active links in route table and cause minimum data loss. Whereas in conventional AODV reliability costs for the decrease in throughput. Static control signal interval in AODV loses some of the breaking link information and provides most of the network's bandwidth for control signals.

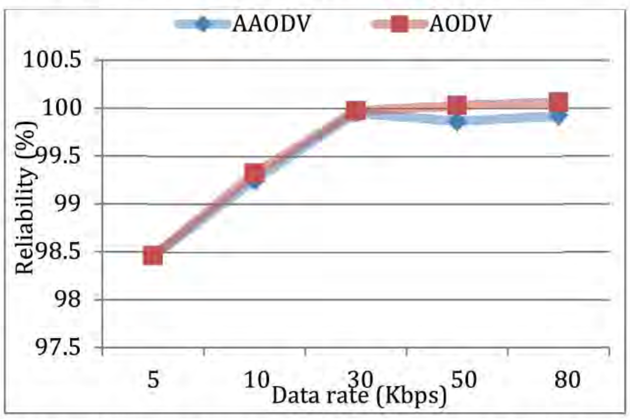

Figure 5, Reliability comparison of AAODV and AODV protocols with slow mobility- Speed 4m/s

f. Energy for Slow Mobile Nodes - Speed 4m/s

Energy Consumption for slow speed mobile nodes moving with rate of 4m/s has shown in Figure 6. Power reduction of both protocols remains approximately the same for low data rate; But as data rate increases energy depletion in AAODV also increases. This increase in power consumption is due to data transmission. The control signal interval is reduced in AAODV at high data rate to have updated link knowledge which reduces its power depletion for control signals; However at the same time the Adaptive AODV provides more data to be transmitted on active link to increase throughput which causes an increase in its energy consumption. So AAODV has a little higher energy consumption for high data rate in mobile network as compare to conventional AODV but with much enhanced performance.

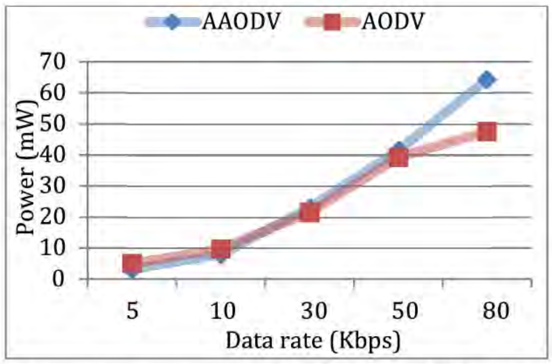

Figure 6, Energy comparison of AAODV and AODV protocols with slow mobility - Speed 4m/s

g. Throughput for Highly Mobile Nodes- Speed 12m/s

Similarly for high speed nodes the throughput of AAODV is higher than AODV throughout the simulation. Result for high speed of about 12m/s is presented in Figure 7. This can be seen from the results that AAODV throughput is 28% better than conventional AODV under high mobile conditions. The high speed nodes require frequent update of their local surrounding to determine active links. In conventional AODV control signal interval is fixed which do not provide network with updated link information for these high mobility nodes. Due to this huge amount of data loss occurs which reduces the efficiency of conventional AODV much lower than low speed and static nodes. The AAODV enhance these results by reducing the control signal interval for these highly mobile networks. The reduced value of these intervals keeps the nodes updated with the surrounding node information hence no stale or broken links is present in node's directory. Also it enhances the performance by providing optimum value of interval at various data rate for high speed nodes. It can be depicted from the results that efficiency of AAODV is far more than the conventional AODV for high speed node using variable data rates.

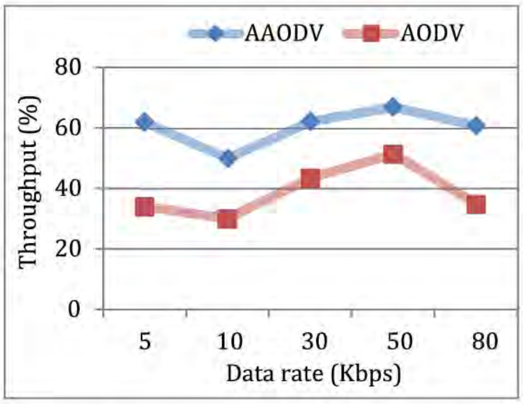

Figure 7, Throughput comparison of AAODV and AODV protocols with high mobility - Speed 12m/s

h. Reliability for Highly Mobile Nodes - Speed 12m/s

Reliability for high speed nodes of 12m/s has shown in Figure 8. From results it is observed that for high speed nodes moving with velocity 12m/s, the reliability of AAODV is slightly lower than conventional AODV. For high mobility the adaptive behaviour of control signal interval is concern with data rate and node speed which effecting the network reliability. Due to high mobility network consume more time in link determination which causes a delay in data transmission. Some of the control signal also loss due to movement of these nodes which in result effect reliability. An additional factor for effecting reliability in Adaptive AODV is it utilize maximum bandwidth for data transmission along with updated link information. Hence this difference of around 0.5 % in reliability is tolerable for AAODV in order to get improved and highly optimized result for network performance.

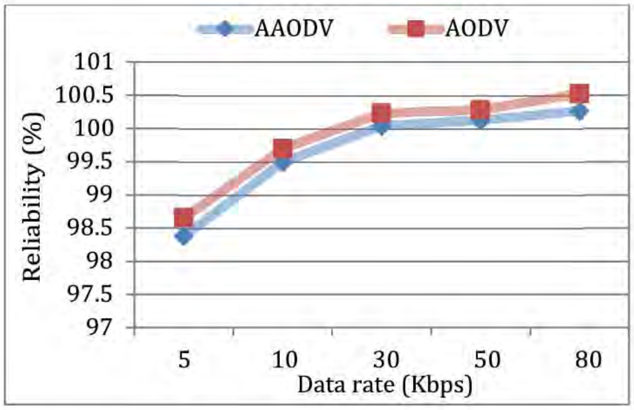

Figure 8, Reliability comparison of AAODV and AODV protocols with high mobility- Speed 12m/s

i. Energy for Highly Mobile Nodes - Speed 12m/s

Energy depletion in node increases more with increased mobility. Node with high speed of 12m/s consumes more energy as compare to static and low speed nodes, shown in Figure 9. With high speed nodes, consumption of energy for AAODV is lower for low data rate. At low data rate the conventional AODV uses more energy by having a large static control signal interval whereas an Adaptive AODV reduces this energy consumption by selecting optimum interval duration. But for high data rate the energy consumption of AAODV is greater than AODV. This increment in energy depletion is due to more data transmission in AAODV at high data rate which yields an effective performance of AAODV under high mobility. This little energy overhead is bearable for AAODV to get an optimize result for network efficiency.

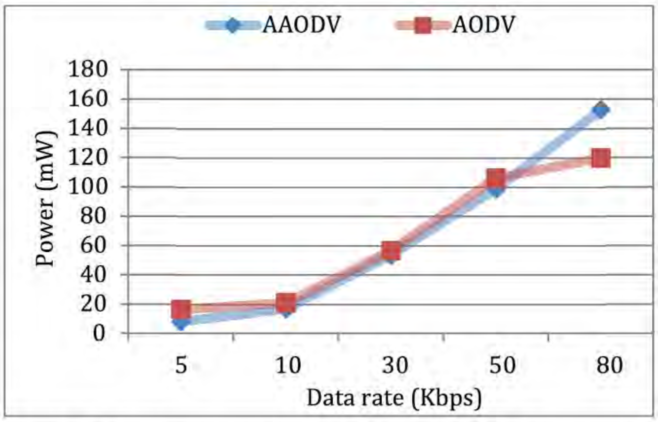

Figure 9, Energy comparison of AAODV and AODV protocols with high mobility - Speed 12m/s

VI .Conclusion and Future Work.

In this paper a novel routing algorithm AAODV is presented which is to the best of author's knowledge is the first of its kind. The results shows that Adaptive AODV provides more effective and reliable network performance with less complexity and overheads. Detailed simulation and analysis of the proposed protocol shows that AAODV significantly outperforms in terms of throughput, reliability and energy consumption than the conventional AODV protocol under both static and mobile scenario with varying data rates. Even with mobile nodes AAODV can gives up to 28% increased throughput in comparison with conventional AODV with maintaining reliability factor above 98. This enhanced performance of AAODV can be utilized with any scalable network. In Future the performance of AAODV can be enhanced much by considering more factors for adaptive control of Signal Interval.

In future the work will be implemented on TELOS B mote and calculated and measured results will be compared in hardware implementation scenario.

References

[1]. Rodolfo Oliveira, Miguel Luis, Luis Bernardo Rui Dinis, Paulo Pinto, *"The Impact of Node's Mobility on Link-detection based on Routing Hello Messages"*, This full text paper was peer reviewed at the direction of IEEE Communications Society subject matter experts for publication in the WCNC 2010 proceedings.

[2]. Raphael Ernst, Peter Martini, Dept. of Computer Science 4, Germany, *"Adaptive HELLO for the Neighborhood Discovery Protocol"*, 37th Annual IEEE Conference on Local Computer Networks LCN 2012, Clearwater, Florida

[3]. Josias Lima, Jr, Thiago Rodrigues, Rodrigo Melo, Gregório Correia, Judith Kelner, and Eduardo Feitosa, *"On the Tuning of Wireless Heterogeneous Routing"*, 2013 IEEE 24th International Symposium on Personal, Indoor and Mobile Radio Communications: Mobile and Wireless Networks.

[4]. Ian D. Chakeres, Elizabeth M. BeldingRoyer, *"The Utility of Hello Messages for Determining Link Connectivity"*, IEEE/Wireless Personal Multimedia Communications, 2002. The 5th International Symposium on Date 27-30 Oct. 2002

[5]. Krunal Patel, Tejas Vasavada, Mayur Vegad, *"Effect of Hello Message on Performance of Ad-hoc On-demand Routing Protocol"*, National Conference on Recent Trends in Engineering & Technology.

[6]. Tahiry Razafindralambo, Nathalie Mitton, *"Analysis of the Impact of Hello Protocol Parameters over a Wireless Network Self Organization"*, hal-00384004, version 1 - 14 May 2009

[7]. Essam Natsheh, Adznan Jantan, Sabira Khatun, and Shamala Subramaniam, *"Adaptive Optimizing of Hello Messages in Wireless Ad-Hoc Networks"*, The International Arab Journal of Information Technology, Vol. 4, No. 3, July 2007

[8]. Datuk Prof Ir Ishak Ismail & Mohd Hairil Fitri Ja'afar, *"Mobile Ad Hoc Network Overview"*, IEEE 2007 ASIA-PACIFIC CONFERENCE ON APPLIED ELECTROMAGNETICS PROCEEDINGS December 4-6, 2007, Melaka, MALAYSIA

[9]. Charles E.Perkins, Elizabeth M.Royer, *"Ad-hoc On-Demand Distance Vector Routing"*, Mobile Computing Systems and Applications, 1999. Proceedings. WMCSA '99. Second IEEE Workshop

[10]. Ian D. Chakeres, Elizabeth M. Belding-Royer, *"AODV Implementation Design and Performance Evaluation"*

[11]. Zhenhui Zhai, Yong Zhang, Mei Song, Guangquan Chen, *"A Reliable and Adaptive AODV Protocol based on Cognitive Routing for Ad Hoc Networks"*, IEEE/ Advanced Communication Technology (ICACT), 2010 The 12th International Conference in Feb. 2010

Automatic Control of a Steam Driven Power Generator to Maintain Steam Pressure in Turbine

Rizwan Zameer
Department of Mechanical & Aerospace Engineering
Air University, Islamabad, Pakistan
200566@students.au.edu.pk

Syed Irtiza Ali Shah
Department of Mechanical & Aerospace Engineering
Air University, Islamabad, Pakistan
irtiza@mail.au.edu.pk

Huzaifa Bin Hanif
Department of Mechanical & Aerospace Engineering
Air University, Islamabad, Pakistan
200534@students.au.edu.pk

Majid Mehmood
Department of Mechanical & Aerospace Engineering
Air University, Islamabad, Pakistan
majid.25mehmood@gmail.com

Abstract—Load Frequency Control (LFC) is a crucial factor responsible for ensuring the stability and efficiency of power systems, thereby facilitating the production of high-quality electricity. The primary objective of LFC is to maintain the system frequency at the ideal required output level, ensuring the unified operation of the entire system. LFC plays a critical role in regulating the frequency against variations induced by diverse load disturbances. Integrating intelligent techniques into the frequency control mechanism has become imperative to optimize power generation. The core function of Load Frequency Control involves governing the speed of generators to maintain a balance between the demanded load and the power generation within each control region. This process aims to minimize deviations in system error, both in steady-state and transient conditions, effectively reducing these errors to zero. Notably, significant advancements have been made in developing controllers based on various intelligent techniques. Given that the frequency of load fluctuates over time, selecting the optimal value poses a challenge. Conventional controllers often exhibit undesired overshoot in response to step inputs and result in unwanted settling times. These limitations are particularly evident when dealing with singularities in the speed of governor systems, such as steam valve position rate limits. To address these challenges, numerous techniques have been proposed and implemented in the past, with some proving highly effective in maintaining system stability. In this context, our approach involves designing an automatic feedback response controller for the load frequency control model. This controller aims to ensure system stability by effectively rejecting frequency disturbances arising from system dynamics. Its primary function is to regulate the speed of the governor shaft to control the steam valve position, thereby maintaining turbine steam pressure and subsequently, the generator's shaft speed. The design of this automatic controller hinges on two fundamental requirements: stability and transient response. The control model is engineered to be robust, capable of reducing steady-state error to zero through a closed-loop feedback mechanism. By modulating the speed of the governor system, the controller compensates for steady-state errors until the output matches the input, ultimately restoring system stability.

Keywords: — Power system, steam driven power generator, Load frequency control, steam turbine, single area LFC.

The terminologies used in this paper are:

LFC	Load Frequency Controller
AGC	Auto-power Generation Control
$T_g(s)$	Time constant of Governor
$T_t(s)$	Time constant of Turbine
$T_P(s)$	Electrical System Time constant
K_p	Electrical System Gain
$G_c(s)$	Controller transfer function
$R(s)$	Input variable of T(s) (Command)
$C(s)$	Output variable of T(s) (frequency)
$T(s)$	Equivalent transfer function

$G(s)$	Plant transfer function
s	Laplace variable
G_g:	Transfer function of Governor
G_t:	Transfer function of Turbine
G_m:	Generator and load transfer function
U	System input in state-space
Y	System output in state-space
$c(t)$	System input in time domain
ω_n	Natural frequency
ζ	Damping ratio
K	P-controller gain

I. Introduction

The primary function of the system is to keep a continual equilibrium between load generation and load demands. In real-time power operations, disturbances due to load effect in varying the required frequency value. The load frequency of the plant system is controlled by AGC (Auto- generation control), also called as load frequency control LFC is an important factor in working of load power system and control to generate enough and consistently dependable high-quality electric power by keeping the frequency of the system within appropriate limits.

II. Literature Review

Many revisions and researches have been done on the load frequency control (LFC). Different controllers were used but the PI controller is most widely used for LFC [1]. A benefit of employing a PI controller is that it uses a close-loop feedback method to lower the steady state inaccuracy. Due to the distinctive properties of the speed of governor system, which have a significant impact on LFC behavior, maintaining the necessary frequency accuracy is challenging. When there is speed- governor singularities, for instance steam flow rate parameters on valve high-quality, the standard PI LFC approach doesn't offer an acceptable control output (Generation Rate Constraint). It is generally known that traditional load frequency control cannot generate satisfactory control performance when the speed governor system has singularities, such as rate restrictions of steam on valve position. The governor, which may be mechanical, hydraulic, or electronic, holds mass flow rate of vapors in turbine to regulate the steam turbine.

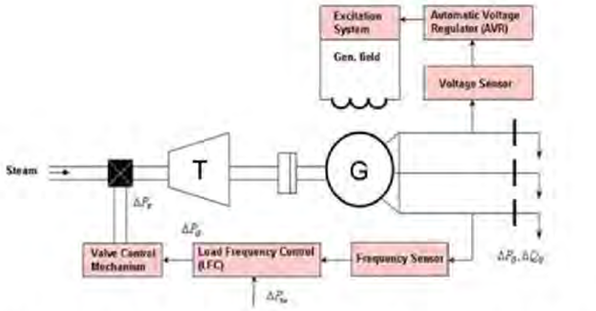

Fig 1. Components of AGC and explanation of their operations [1].

The best value is difficult to choose since load frequency changes over time. The traditional PI controller frequently overshoots a step input instruction by an excessive amount. An expanded integral control approach with Generation rate control (GRC) is used to control the speed governor of system for the LFC scheme to prevent these overshoots of the typical PI controllers [2]. The typical LFC architecture was unable to provide the needed performance because to issues with the speed governor. A prolonged integral control was created with the purpose of combine GRC and proportional plus integral (PI) regulate of speed governor system. To mitigate the effects of accuracy and steady-state faults, the prolonged integral control technique relies on the use of a fading factor. The decaying factor ought to adapt to the system's changing aspects. This research estimated the fading feature and the loop gains based on degree of deviation and the response measure to attain the system's optimal output.

Extended integrated control, for power system of the speed governor system is suggested for oscillations of power system stability [3]. Fundamental reason for the oscillations in the power system is the extra locomotive energy that is kept in the generator throughout unsteady period. There is a valve to control and regulate the extra energy is the simplest technique to accomplish system stabilisation. The speed-governor system is under PI control for the LFC (Load Frequency Control). It is clear that the conservative PI LFC approach does not generate control output that is satisfactory when the speed governor's limits, for instance, those on regulator location and GRC, are taken into consideration. For the control of the speed governor using PI, an extended integral control is being designed to address all of these problems and flaws. The recommended controller, which is grounded on prolonged integral control, beats the conventional PI type controller in terms of control action, according to simulation data.

For frequency. control of power system, an innovative PID controller design with the same parameters and minor changes was proposed [4]. An innovative technique was created for the PID controller's systematic tuning. It is built on the extreme peak-resonance theory and is illustrated by a graphical version of the Nichols chart. This controller's straightforward design guarantees that the system is operating properly. This novel load frequency controller's calculations and results were contrasted with those of the traditional PI controller, demonstrating an improvement in system damping.

A different technique for fine-tuning the PID settings of the load frequency controller was created. This tuning technique is based on the Quantitative Feedback Theory-based stable controller design (QFT) [5]. This QFT-based PID controller improves the standard PI controller by increasing the hindering of the system following a step change in load. The closed loop function in QFT desires to cover a range of discrete frequencies in order to meet specific performance requirements. These requirements are defined in accordance to the tolerance intervals that the extent response of the feedback transfer function must fall inside. It is anticipated that the controller will handle both the governor's and the turbine's transfer activities. The ultimate controller equations are:

$$G(s)=G\_1\ (s)\ G\_2\ (s)$$

In which $G_1(s)$ is the turbine and $G_2(s)$ represents governor function, and are the key parameters in PID as presented in Figure 2.

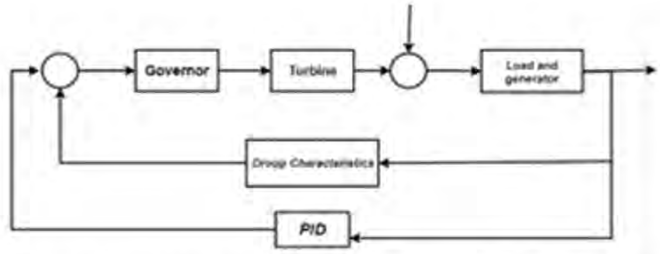

Fig 2. The Closed-loop Block diagram of system with PID control of power system [5]

The equations of modeled system consist of three main models which are given as:

$G_g(s) = \frac{1}{0.2s+1}$ is governor's Transfer Function.

$G_t(s) = \frac{1}{0.5s+1}$ is the turbine's Transfer Function

$G_m(s) = \frac{1}{10s+0.8}$ is the Load's Transfer Function

Fuzzy logic-based control is an intelligent technique used to regulate the required or ideal limits for extended integral control [6]. This approach is an extension to the work that Moon et al. [2] proposed be done to enhance Extended Integral Control for Frequency. A crucial point is that the degree of the frequency deviation must be taken into interpretation when adjusting the time-varying decaying factor of the extended integral control. The extended integral control's effectiveness is strongly influenced by the decaying factor. To obtain optimal or almost ideal performance, the fading factor and feedback loop gains must be transformed very fast in reaction to deviates in the system dynamics. To respond to shifting feedback signals, the fading factor may be efficiently identified using fuzzy set theory. According to the findings of simulations, a fuzzy logic-based controller performs better at controlling than a traditional PI controller. Frequency management is a critical steadiness requirement in power systems. The constancy of the power system depends on constant frequency and dynamic power balance. Frequency is influenced by the active power balance. A power system's frequency can't be kept at its appraised value if the active power changes, and oscillations in both power and frequency increase.

Another intelligent method for the LFC problem in power systems that addresses these issues is the LFC-based adaptive PID controller, which uses techniques from Artificial. Neural. Networks. (ANN) and Neuro-Fuzzy. Inference. Systems (ANFIS) guided by Genetic Algorithm (GA) [7]. PID controller settings is modified offline by means of GA to reduce basic error squares over an inclusive series of load fluctuations. Both ANN and ANFIS are run on the data received from GA, and the results provide the PID controller's ideal values for the given range. The adaptive PID Load Frequency Control might sustain ideal performance over a wide series of loads, according to simulation results of the devised approach.

An integral controller is used in conventional LFC. The system's performance might be negatively impacted by a high integral gain, leading to significant oscillation and unsteadiness. So, integral gain should be adjusted to a level to get a necessary transient response and little overshoot in the active behaviour of the whole system. According to stability analysis of the current control laws, constraint distinction is not a major problem, but un-model subtleties in stable load frequency controller design need more attention. A stable load frequency control approach is then provided based on the nonlinear subtleties of the system to avoid the impacts of generation rate constraints (GRC) [8]. Outcomes from simulations display how effective the design strategy and the anti-GRC setup are.

Another control system having an advance method for tuning parameters is to plan a new advanced PID controller for the power system. There are many numbers of ways and techniques through which we can tune the constraints of PID control to get the required response of our system. The approach used to attain the system constraints is solving the systems transfer function using the Laurent series [9] instead of other conventional methods. LFC behaviour of a single area is studied in this research. In this work, a relay feedback mechanism is used to represent the changing behaviour of the power system. It is possible to gauge the steadiness of LFC using Kharitonov's theorem. The proposed method greatly boosts control effectiveness, particularly when it comes to removing disruptions. This technique demonstrates that the projected PID controller with a novel relay feedback mechanism performs better than previous suggested techniques. Block Diagram of single power area system is given as in Fig 3:

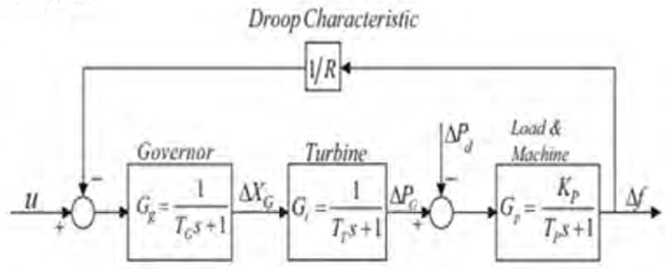

Fig 3. The Block Diagram of single area power control system [9]

The system's equation modelling is given as;

$$\frac{y}{r} = \frac{G + GG_c G_m e^{-\theta_m S}}{G_m(1 + GG_c)}$$

When the model value matches system dynamics, above equation reduces to:

$$\frac{y}{r} = e^{-\theta_m S}$$

The system closed-loop model used for LFC is,

$$G = \frac{G_g G_t G_p}{1 + \frac{G_p G_t G_g}{R}}$$

The above equation can be shown by 2nd order transfer function,

$$G = \frac{ke^{-\theta_m S}}{(T_1 s+1)(T_2 s+1)}$$

Md Nishat [10] proposed a new technique to frequency domain controller design which is based on the direct synthesis (DS) technology. To acquire PID parameters, the DS controller and PID controller's frequency responses are matched. In order to get a set of linear algebraic equations, matching is performed at two separate low-frequency sites. The system obtains the PID parameters by the solution of these equations. Points are selected for proper frequency matching and effective control system performance at the low points of the frequency response spectrum in order to match both frequencies. This method considers nonlinearity like the generating rate constraint (GRC). The recommended technique is not constrained by the system model's complexity or structure. When creating the transfer function for necessary general reference model, system subtleties and performance requirements are taken into consideration.

LFC (Load Frequency Control) design approach grounded on fractional order control is created by means of Kharitonov's theorem [11]. Instead of using a single fixed value for each system parameter, this strategy is built by taking into account a range of values. Results indicated that this method helps make the controller very stable against a greater variety of parameter fluctuations when associated to previous insignificant controllers. The parameter alterations up to which the controller should properly operate using this manner is entirely up to the design engineer. By preventing harm brought on by unexpected increases in any system parameter, this technique makes the system secure. According to the results, the recommended controller operates more effectively and can maintain system stability over a larger range of changes in system parameters.

For both single as well as interconnected multi area power systems, additional PID controller using the Internal Mode Scheme (IMC) is presented in [12]. An integrated two-degree-of-freedom IMC architecture is proposed for frequency management of power plant system comprising non reheated, reheated, and hydro turbines. It was done to reduce the influence of the unwanted poles of the disturbance, which increases the closed-loop system's efficacy at attenuating disturbances. The performance and resilience of the system are controlled by PID's two tuning parameters, according to simulation findings for both single-area and multiarea power systems.

A networked nonlinear power system's load frequency is being controlled with the goal of doing so while taking input delays into consideration, [13] is related to the development of an adaptive type. 2 fuzzy PID also written as T2FPID controller. The control system may become unstable due to the input delay, which is usually increased by communication connection failure and actuator operating lag. This work has generated adaptive laws for modifying the output grading factor of the controller and tested the stability of the produced laws by utilizing Lyapunov-Krasinski written as L-K theorem. To regulate the nth region of power system, the T2FPID has nine basic rules established.

TABLE 1. BASE RULES OF T2FLS CONTROL FOR nth AREA [13]

r_{2i}	r_{1i}		
—	N	Z	P
N	NL	NM	Z
Z	NM	Z	PM
P	Z	PM	PL

The adaptive process corrects for any errors, and these rules encompass all control activities needed to decrease system error to zero.

It is suggested to use a PID controller with the firefly method to regulate frequency control in [14]. This firefly method is used to test PI and PID in LFC under step load disturbances. Its advantage is established by comparing the simulation results to those from other traditional approaches. By altering the system constraints from their minimal values, sensitivity analysis is supported to better explain the resilience of the technique. It might be used in a real-world situation. It is challenging to manage the pressure using traditional controllers because they cannot handle delay time, steady-state inaccuracy, and transient response. With the aim of completing this task, a hybrid system is used in conjunction with traditional controls [15]. In this optimised hybrid system, a PID controller is there for the control of system and a fuzzy controller (a fuzzy controller is a discrete time variant of a regular PI controller). what is typical. Integral controllers were employed to avoid the high steady-state error that a proportional controller creates, but they had the drawback of making the process slower. Therefore, a hybrid controller that combines a traditional PID controller with a fuzzy controller was proposed. Future experts will see hybrid countertrolled by the model base controller as the optimum method for decreasing overshoot time and convergence rate.

In this study, a novel, reliable PI design is created using the Kharitonov theorem. The suggested method seeks to raise the stability margin as well as the transient responsiveness [16]. The Kharitonov theorem's zero-exclusion condition are used to prove robust stability and calculate the robustness ranges. Simulations which are time based are used to produce the LFC system's transient behaviour, and ITSE is used to gauge its transient performance. A control cost function is created that takes stability margin and transient performance into account in order to optimise PI profits.

When it comes to the examination of a system's stability, the PID-derivative filter has been deemed to be superior than traditional PID control. The falling of the derivative filter with the PID controller serves as the foundation for this suggested controller. The two-area linked power system's stability has increased thanks to presented controller. To show the applicability of PID-derivative controller, several situations have been looked at and compared to alternative methods. The recommended derivative controller increased the stability of the system, according to experiments, when compared to the traditional proportional, integral plus derivative controller for time domain analysis [17].

PID-derivative filter has been deemed to be superior than traditional PID control. This recommended controller cascades the derivative filter and PID controller. The presented controller has improved the stability of the tie lined power system. Several scenarios have been examined, and PID-derivative controller's effectiveness has been contrasted with other approaches. Experiments showed that the recommended derivative controller, as opposed to the more popular proportional integral derivative controller, enhanced the stability of the system in time realm analysis [18].

The generalised active control for the rejections of disturbance (GADRC) approach is investigated for frequency management in single and multi-area systems. The GADRC system is converted into an internal two-degree of freedom model form using a bandwidth tuning technique [19]. The performance through GADRC is transitory, with minor undershoot, a rapid settling time, and minimal values for performance measures. By contrasting the disturbance neutralisation capabilities and performance measurements of these procedures with other techniques and more traditional ways that are known to exist in the literature, the validity and efficacy of these techniques are confirmed.

Another straightforward method for constructing fractional order type controller employs the internal control of model strategy to address the problems in Load Frequency Control (LFC) of power generation systems. The CRONE concept, model-order reduction, and the FO filter are used in the internal model control IMC framework by the suggested technique to build a robust controller [20]. Both two-area linked systems and single-area electricity systems can employ this technique. The only frequency domain requirements required for the recommended control architecture are phase margin and gain crossover frequency.

Additionally, automated LFC or AGC of power systems using the two degree of freedom fractional-order PID (2- DOFFOPID) controller is being researched [21]. Automatic generation control (AGC), which responds to disturbances and other steady-state faults in the system's load frequency, regulates the active power (generator output). Three thermal power systems with uneven areas are being used for the first time using two degrees of freedom fractional order. The Firefly algorithm was used to manage the different PID controller and governor settings. The durability of the suggested controller under different numbers of loading conditions and the inertia constant is confirmed by a sensitivity investigation. Additionally, this controller performs well in the existence of step load disturbances and arbitrary load patterns with a greater degree.

Automatic. Generation. control (AGC). is recognised as the most extraordinary solution for supplying end consumers with high-quality electric power in the ever-expanding scope and difficulty of the energy system. [22] presents a brand-new expert technique called the hybrid. Fuzzy. Fractional. order proportional. Integral fractional. order proportional. derivative. (FFOPIFOPD) controller. ICA is used to optimise the proposed controller's settings using the ISE. error criteria. Both single-area and multiple-area linked power networks can use this technique. Studies show that this controller delivers higher dynamic performance over alternative techniques. Even with significant variations in system characteristics and other generational constraints, the controller is dependable and capable of performing effectively. Through a connected power network, the exchange of electricity is controlled, and the frequency is changed to stay within the normal range. Since both the active and the reactive loads are dynamically shifting, vibrations are the outcome. Automatic Generation Control may effectively bring the system's oscillations into the usual range (AGC).

For automatic load frequency control, D. Gupta has developed a brand-new heuristic-based hybrid optimization technique[23]. The Firefly Algorithm (FA), Particle Swarm Optimization (PSO), and Gravitational Algorithm are the three optimization approaches that make up the bulk of the recommended optimization strategy (GSA). The error in the system was decreased in order to change the PID controller's settings. The disturbance step load change was taken into account while evaluating the system's performance. The experimental findings were compared to those of other optimization approaches to evaluate the performance of this algorithm, and they demonstrate the efficiency of this heuristic-based hybrid optimization methodology.

Due to rising worries over the plodding depletion of fossil fuel assets and the ecological issues caused by their releases, the power grid now takes the potential of alternative/renewable energy sources into account. As an alternative controller for secondary load frequency regulation, the FPD/PI-PD controller is provided. It is a well-organized combination of fuzzy logic based PD and cascade PI plus PD controllers [24]. Compared to traditional PI or FPID controllers, it offers great stability in response to frequency changes. Frequency load management increases the performance of a closed loop system by establishing a non-linear connection between input and output. By establishing the function and laying out the replies by controlling integral error, the optical set of secondary control is the primary focus. These traditional controllers therefore attain excellent dynamic stability.

Frequency deviates significantly from the ideal tie line due to the erratic input and output of system power and load disturbance. The standard PI or PID controller does not provide the results needed to operate the system under these circumstances. The system becomes unstable as a result of a significant frequency variation caused by the disorder in the inertial output. For microgrid frequency control (MG). To address this issue, [25] advises an efficient load frequency controller. Using a grasshopper optimization technique, the controller modifies the PID controller's parameters (GOA). The recommended approach balances generation and load in a hybrid microgrid set-up using diesel engine generators and redox flow batteries. This approach improves responsiveness with regard to timing, settling time and also peak overshoot when compared to other controllers.

Tie-lines link the large-scale power systems that make up the control rooms. These tie-lines are used for interarea support in exceptional circumstances as well as power exchange between the control regions. Voltage and frequency are the key determinants used to assess an electrical system's power quality. A crucial issue is automatic generation control (AGC), particularly in situations involving interconnected systems, for the effective operation of power systems as well as for the delivery of superior energy to customers. [26] provides a method for refining the AGC performance of multi area power systems by building fuzzy classical controller based on the output scaling factor (SF). In the initial application of the competitive algorithm with imperialism, the output SF of the fuzzy proportional integral (FPI) controller is optimised using the integral. of squared. error. criteria (ICA).

To solve the issue with the AGC of the power system, Messam introduces a unique integrator and derivative action fuzzy operational integral derivative (PID) controller, also known as the fuzzy PID controller [27]. Using the recently developed and successful metaheuristic cuckoo optimization strategy (COA) to create the suggested structured controller as efficiently as feasible is one of the study's goals. The optimization work for modifying the constraints of the suggested controller is finished using the cuckoo. Optimization. Algorithm. (COA).

The demand for power on a regular basis continues rising. The most tough part is guaranteeing that customers can admittance dependable, first-class electricity irrespective of the weather. Automatic. Generation. Control. (AGC), which keeps the correct output power and required frequency in spite of instabilities in load, is used to accomplish this. Instead of using a conservative controller, To maintain the load frequency at the desired level, an effective hybrid PID fuzzy AGC based on the simulated tempering controller technique is developed [28]. A judgemental study was performed between the suggested controller and the PID controller. Both controllers' settings were created utilising simulated. annealing (SA) methods in order to get the top dynamic performance. The PID fuzzy. controller performed significantly superior than a conventional PID controller.

In the broad, interconnected power networks, a control area or region stands in for a coherent group of generators. Tie-lines connect the various locations. In order to move energy between the two regions and to offer inter-area assistance in the event that the power system encounters unexpected circumstances, tie-lines are utilised. The tied-line power response plus frequency response of the linked regions have been compared using the peak value of overshoot, peak value undershoot, and settling time measures. When output of a fuzzy logic controller is contrasted with that of a conventional one like a proportional derivative plus integral (PID) controller [29].

To maximise the input scaling and output scaling of aspects of the logic controller, is suggested using a harmony search technique (HSA) while designing the fuzzy logic power system stabiliser (FPSS) [30]. Optimization problem is viewed as the objective function lowering of integral square-error for single machine and multi machine power systems. The fine system stabiliser is formulated using a nonlinear model of a single area power system as well as a two-area system. To achieve resilient stability, the optimization issue is tackled using parameter constraints.

A. Literature Review Summary TABLE

Reference No.	Approach/Technique	Findings/Comments
1	The load frequency is controlled by a PID controller.	PID controller has an advantage in that it reduces the steady state and settling time by using a closed loop feedback mechanism.
2	An extended integral control-based controller is cast-off to control the frequency.	The simulation studies successfully presented the application of an integral control to minimize the excessive overshoot of a step input command.

Reference No.	Approach/Technique	Findings/Comments
3	An expanded integral controller was used in a new technique to regulate a speed. governor system for mitigating power system oscillations.	Simulation studies demonstrated that the system is functioning as intended and that the recommended controller has enhanced the system's performance.
4	Based on the maximum peak-resonance hypothesis, a novel PID controller was created for load frequency management.	The controller's design is straightforward. It enhances system damping and effectively regulates the governor's speed.
5	Based on the Quantitative Feedback Theory, a novel design and tuning strategy for LFC was investigated (QFT).	The suggested design is utilized to improve the response of the system against a step change in load since it performs very well than a traditional PI class controller.
6	The needed or ideal parameters for extended integral control are chosen using fuzzy logic-based control.	The extended integral control system's decaying aspect is found using this method. Simulation experiments were successful in demonstrating the efficacy of this strategy.
7	ANN and ANFIS based system were presented for systems stability.	A comparison between the results of the simulation and the adaptive PID Load Frequency Control showed that it could continue to function at its best under a variety of loading.
8	A stable approach is utilized for the control of frequency to overwhelmed effects of generation rate constraints (GRC) and unmodeled dynamics of the controller.	Computer simulations demonstrate how well the LFC can reject disruptions brought on by the GRC and other changes of the control system.
9	Laurent series is castoff to study the parameter of the system by solving the transfer function.	The suggested technique improves control performance significantly, especially in neutralizing disturbances.
10	The direct Synthesis approach (DS) is used to model a control design.	The design of controller is very simple and algebraic equations are obtained by matching the frequency at two different points through Direct Synthesis. And these equations are very easy to solve and give information about the performance of the system.
11	Kharitonov's theorem is used to develop a method of controller design that emphasizes fractional order control.	Simulation outcomes demonstrates that the suggested controller performs well and can stabilize the system for a variety of system parameter modifications.
12	The Internal Mode Scheme (IMC)-based PID controller design is created.	This design of IMC is 2 DOF based which was adapted to reduce disturbances to enhance the performance of system. An

Reference No.	Approach/Technique	Findings/Comments
		additional degree-of freedom was set to eliminate the outcome of the undesirable poles of the disturbance.
13	Lyapunov– Krasovskii (L-K) theorem was used in this study to test the firmness of the developed T2FPID and to maintain the controller output stable.	The major benefit of the controller is its easiness in terms of execution. The simulation studies successfully presented the application of an adaptive control solution for controlling varying input delays.
14	It was presented how to regulate frequency of loads using a PID controller based on the firefly algorithm.	Controller is tested by changing the parameters of system from their nominal values. Comparison of the simulation results with other conventional methods proves its superiority.
15	This solution solves the issue of significant steady-state errors by using a hybrid control system approach. The hybrid system combines a PID controller with fuzzy controller.	Pressure process control is utilized to test and illustrate usefulness of the hybrid fuzzy PID controller.
16	The Kharitonov theorem approach is used in this study to provide a new stable PI controller design to improve the robustness criteria and transient response.	The comparative study of the presented control strategy proved the reasonable stable performance of control for the varied range of the system.
17	PID-derivative Load frequency controller instead of a simple PID was studied. The PID controller and derivative filter are cascaded in this controller.	The analysis of the suggested control shows that the application of the PID-derivative filter controller has resulted in an important improvement in system stability.
18	The approach used in this study is to use some of the existing LFC controllers together to control the load frequency more effectively and smoothly.	It has been the goal of several research, including those employing single- and multiarea power systems, to confirm the accuracy and efficacy of the proposed technique.
19	This work studies the generalized active. disturbance. rejection. control. (GADRC) scheme for frequency management.	By contrasting disturbance rejection capacity and performance metrics of this methodology with those of other established techniques, the validity and efficacy of it are confirmed.
20	Another modest approach to designing a fractional. order. controller uses the internal model control technique. The suggested method uses the concept of the CRONE principle,	Both single and two interconnected areas systems can employ this approach. Crossover of phase margin and gain. The only frequency domain is frequency. requirements for the proposed control design.

Reference No.	Approach/Technique	Findings/Comments
21	The automatic LFC of power systems is presented in this study using a 2 DOF fractional PID (2-DOF-FOPID) controller.	This controller performs well when faced with step load disturbances and random load patterns that are more severe.
22	The hybrid FFOPI-FOPD controller is a novel professional method that is recommended.	Studies proves that the suggested controller outperforms rival strategies in terms of dynamic performance. The controller is reliable and can function well even when the system parameters and other generational limitations vary.
23	A novel hybrid optimization method using Firefly. Algorithm., Particle. Swarm. Optimization, and Gravitational. Search. Algorithm. that is based on heuristics. (GSA).	The usefulness of this heuristic-based optimization strategy is established by comparing the experimental results with those of other optimization strategies to calculate the performance of this algorithm.
24	A controller for secondary load frequency regulation is utilized which is combination of fuzzy PD, PI plus PD control approaches.	These traditional controllers provide strong dynamic stability for secondary load frequency regulation.
25	In order to regulate frequency of a microgrid, a sophisticated controller based on the GOA for fine-tuning the PID controller's settings was suggested.	Simulation experiments showed that this approach, in comparison to alternative controllers, enhances responsiveness in terms of time, settling time, and overshoot.
26	Two area electrical power systems' AGC conduct is improved by using a fuzzy approach based classical controller that is based on the output scaling factor (SF) technique.	To demonstrate the recommended method's resilience to significant changes in system characteristics and the amount or location of step load disruption, a sensitivity analysis is conducted.
27	A new fuzzy PID controller with filtered derivative action is suggested based on the cuckoo optimization strategy.	Time domain simulation results demonstrate that when compared to other current solutions, created secondary controllers offer an adequate degree of performance and stability.
28	Instead of using a traditional controller, an efficient hybrid PID-fuzzy AGC based on the simulated annealing control approach is created to keep the load frequency at a desirable level.	The proposed controller and the PID were contrasted in a comparative study. To provide the optimum stable performance, the settings of both controllers were created utilizing simulated annealing approaches.
29	Controlling the frequency and fluctuations of electricity in the variations using a fuzzy logic controller.	Results from this fuzzy controller were compared to those from a traditional PID, and it was discovered that system's reaction was quicker.
30	The HAS method is utilized to construct	The advantage of the proposed HSFPSS is

Reference No.	Approach/Technique	Findings/Comments
	the system stabilizer and the fuzzy logic controller's input-output scaling factors should be optimized.	shown by comparing the speed response performance of the system in terms of performance.

III. Methodology

We aim to modulate the load frequency of steam-driven power generation system as the load demand changes by controlling the governor parameters. The load demand in power system is always changing. The power input essential also fluctuate in line with it. The speed governor mechanism, supported by supplementary techniques for accurate control, is used for the frequency regulation.

Governor: The primary dependence of power system is on the synchronous generator and its reliable functioning. This loop of frequency control is an essential control loop in the system. Speed of generator shaft is sensed by feedback mechanism and it regulates the stem intent to the turbine accordingly by consoling steam valve. The explanatory diagram of the working of whole system is presented in Fig 4.

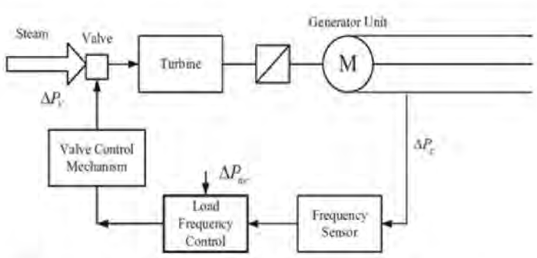

Figure 4. Block Diagram of Load Frequency Control System presenting all the components of system

Basic Principle: The elementary principle of Load frequency control is shaft speed is measured and compared to a reference, and the feedback information is used to increase or decrease the power output by adjusting steam intake valve to main turbine.

Power systems' operating conditions are continually changing because of fluctuations in generation and demand patterns, along with changes in the transmission network. As a result, there is a very much difference in the system's small signal dynamic behaviour.

This study is a continuation of a prior paper [5]. Along with designing and analysing its control system, they focused on modelling a load frequency controller. The plant's tiny signal linearized model's parametric uncertainty is what causes the interruptions. In the previous work, the dynamic modelling of the system was completed. We followed up on those findings by designing and analysing a control system.

A. Approach

Modern methods used as controller such as adaptive control have been used in the past to control all Parametric errors in the plant's small signal linearized model. These approaches require either system state information or an effective on-line identification. The whole system state information is also necessary for the modelling of adaptive approaches. So, this model reference technique may be challenging to implement due to the large order of the power system function. To overcome all these problems of adaptive approaches we are using QFT (Quantitative Feedback Theory) based model which have low order power transfer function and is easy to implement.

There are 1. Single-area 2. multi-area LFC systems. But our dealing is with the single area Load Frequency Control by sensing and controlling the speed of the governor shaft. The auto-control system for single area control system is presented in Fig. 5

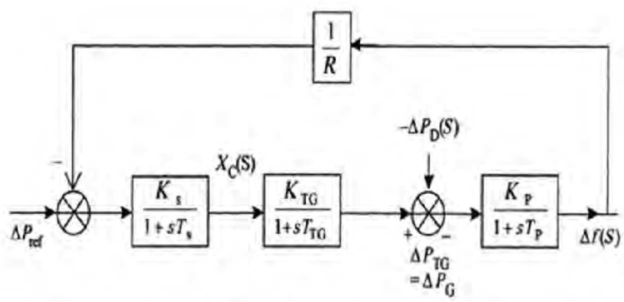

Fig. 5 Block Diagram of Single Area control system [5]

IV. Modelling

Mathematical model of an isolated power system constitutes:

- Speed governor model
- Turbine model
- Generator model

The dynamic modelling of the system is given with detail in [10]. Here is a streamlined and linear block diagram of the control system used to regulate the load frequency of a steam-driven power plant in Fig. 6:

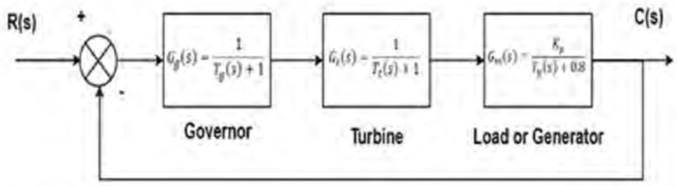

Fig. 6 Block diagram of the system with different components shown[5]

The open-loop transfer function from R(s) to C(s) as in Fig.6 may written as:

$$G(s) = G_g(s)G_t(s)G_m(s)$$

$$G(s) = \left(\frac{1}{T_g.s+1}\right)\left(\frac{1}{T_t.s+1}\right)\left(\frac{K_p}{T_p.s+0.8}\right) \quad [4]$$

Choosing values for the time constants for turbine, governor and generator for the proper implementation of systems. Let $T_g = 0.2, T_t = 0.5, T_p = 10 \; and \; K_p = 10$.

$$G_g(s) = \frac{1}{0.2s+1}$$

$$G_t(s) = \frac{1}{0.5s+1}$$

$$G_m(s) = \frac{10}{10s+0.8} \quad [5]$$

$$G(s) = \frac{10}{(0.2s+1)(0.5s+1)(10s+0.8)} \quad [5]$$

So, the open loop block diagram of modelled system is shown below:

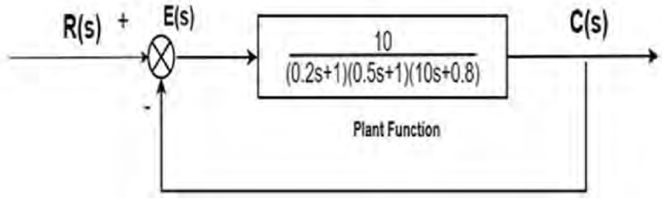

Fig. 7 Open Loop Block Diagram showing plant function of system

Reducing our plant function to 2nd order system:

$$G(s) = \frac{10}{s^3 + 7.08s^2 + 10.56s + 0.8} \quad [6]$$

Characteristic Equation is,

$$s^3 + 7.08s^2 + 10.56s + 0.8 = 0$$

After solving roots are s = -5, -2 and -0.08. Neglecting s = -0.08. so new characteristic equation is;

$$s^2 + 7s + 10 = 0$$

Our new open-loop transfer function is

$$G(s) = \frac{10}{s^2 + 7s + 10} \quad [7]$$

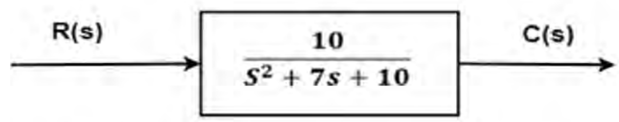

Fig. 8 Block Diagram of Reduced 2nd order transfer function

Now, converting transfer function to time domain using state space modelling:

$$\frac{C(s)}{R(s)} = \frac{10}{S^2 + 7s + 10}$$

$$s^2C(s) + 7sC(s) + 10C(s) = 10R(s) \quad [8]$$

Assuming zero-initial conditions and taking inverse Laplace;

$$\ddot{c} + 7\dot{c} + 10c = 10r$$

Choosing state variables as successive derivatives

$$x_1 = c$$

$$x_2 = \dot{c}$$

Differentiating both sides of these equations and finding values of $\dot{x_1}$ and $\dot{x_2}$

$$\dot{x_1} = \quad x_2$$

$$\dot{x_2} = \quad -10X_1 \quad -7x_2 \quad +10r$$

The output velocity control is:

$$Y = \dot{c} = x_2$$

So, the state space model is

$$[\dot{X}] = \begin{bmatrix} 0 & 1 \\ -10 & -7 \end{bmatrix} \begin{bmatrix} X_1 \\ X_2 \end{bmatrix} + \begin{bmatrix} 0 \\ 10 \end{bmatrix} r \qquad [9]$$

$$[Y] = [0 \quad 1] \begin{bmatrix} X_1 \\ X_2 \end{bmatrix} \qquad [10]$$

The time domain block diagram is represented below;

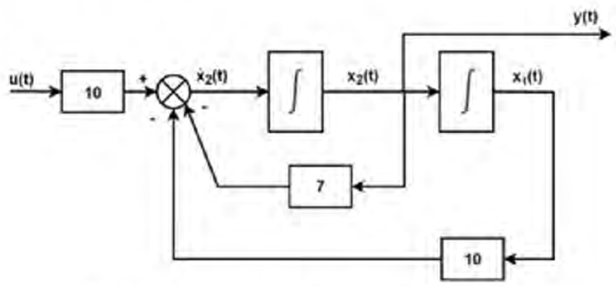

Fig. 9 State space block diagram of the system.

Now introducing the feedback in our system. The block diagram can be represented as:

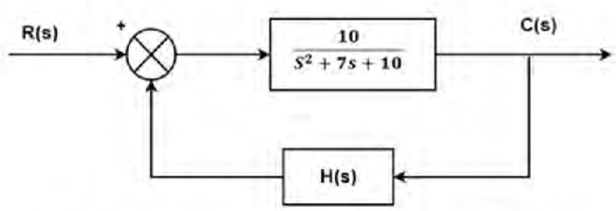

Fig. 10 Closed-loop block diagram with feedback mechanism.

Considering unity feedback (H(s) = 1), the system can be reduced.

Using (A) and (B), the closed loop transfer function is;

$$T(s) = \frac{C(s)}{R(s)} \qquad [11]$$

$$= \frac{G(s)}{1 + G(s)} \qquad [12]$$

So, the closed-loop transfer function can be written as:

$$T(s) = \frac{10}{S^2 + 7s + 20} \qquad [13]$$

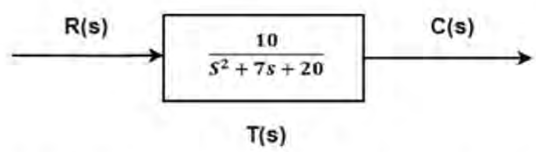

Fig. 11 Block Diagram of Closed-loop Transfer Function of system

V. Implementation

After successful modelling of open and closed loop transfer function of system, next step is the implementation. For the modelling, designing, and characteristics of our system, we have used software like MATLAB, SIMULINK and PID Tuner. MATLAB is mostly used for finding out transfer functions and for observing system transient characteristics whereas Simulink is used for plotting responses against various inputs and for making block diagrams of the system. At the end a very important feature of Mat lab was used i.e., PID Tuner. PID tuner was used to discover the values of gains for P, I and D controllers corresponding to desired characteristics. The values for these gains were varied until the desired response was achieved.

VI. Results

A. Time Response of our system for step input

Using transfer function,

$$G(s) = \frac{C(s)}{R(s)} = \frac{10}{s^2 + 7s + 10}$$

For step input

$$R(s) = \frac{1}{s}$$

$$C(s) = \frac{10}{s(s^2 + 7s + 10)} \qquad [14]$$

Using partial fractions:

$$C(s) = \frac{A}{s} + \frac{Bs+C}{s^2+7s+10} \qquad [15]$$

So, Time response is:

$$c(s) = \frac{1}{s} + \frac{0.6667}{s+5} - \frac{1.6667}{s+2} \qquad [16]$$

Taking inverse Laplace

$$\mathcal{L}^{-1}c(s) = \mathcal{L}^{-1}\left(\frac{1}{s} + \frac{0.6667}{s+5} - \frac{1.6667}{s+2}\right)$$

$$C(t) = 1 + 00.6667e^{-5} - 1.6667e^{-2} \qquad [17]$$

To find Natural Frequency ω_n and Damping Ratio ζ characteristics of a 2nd order system, we transform the transfer function into following form:

$$G(s) = \frac{\omega_n^2}{s^2 + 2\,\zeta\omega_n + \omega_n^2} \qquad [18]$$

By comparing we get:

$$\omega_n = 3.162$$

$$\zeta = 1.10$$

System is over damped because $\zeta>1$ and it has two real poles. Hence Response is of form:

$$c(t) = K_1 e^{-\sigma_1 t} + K_2 e^{-\sigma_2 t} \qquad [19]$$

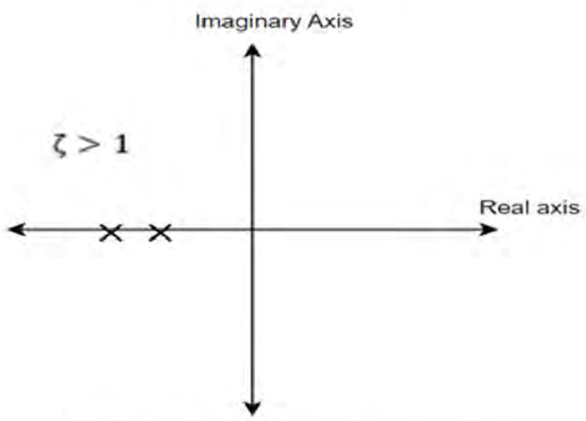

Fig. 12 Pole-Zero Plot of Overdamped system

Using MATLAB, for step input:

```
       RiseTime: 1.2325
   SettlingTime: 2.2112
    SettlingMin: 0.9029
    SettlingMax: 0.9996
      Overshoot: 0
     Undershoot: 0
           Peak: 0.9996
       PeakTime: 4.2183
```

Fig. 13 Characteristics of system calculated using MATLAB

Now testing the system against multiple inputs. All the responses will be plotted and for each response will be discussed pros and cons.

1. For step Input

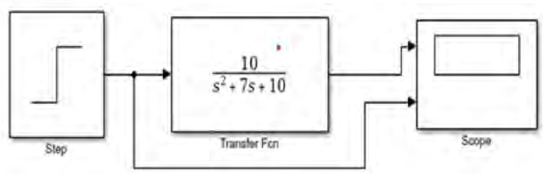

Fig. 14 SIMULINK Block Diagram of transfer function with step input

Fig. 15 Response Plot of system against a unit Step Input

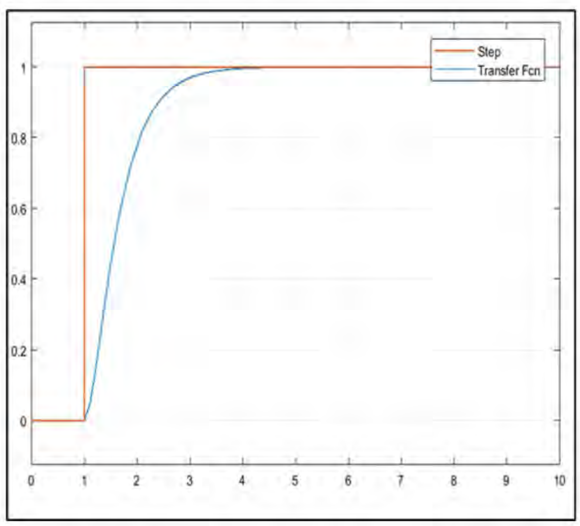

The output response of the system follows the step input precisely but the settling time needs to be improved. Its mean that our system is good to go with some characteristics to be improved.

2. For Parabolic Input

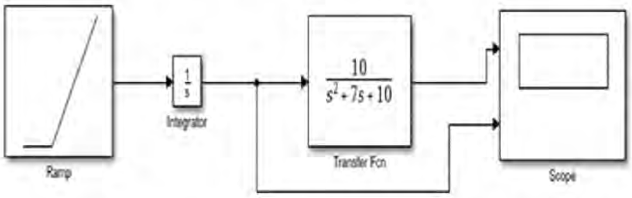

Fig. 16 SIMULINK Block Diagram of Parabolic Input

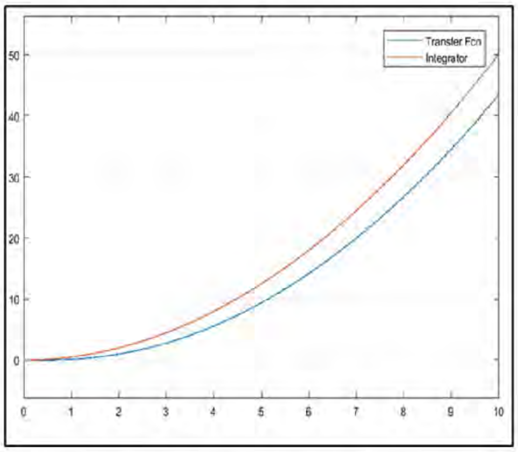

Fig. 17 Response Plot of system against a Parabolic Input

he system is trying to follow the command but the response is lacking behind the input command hence causing steady state error.

3. For Ramp Input

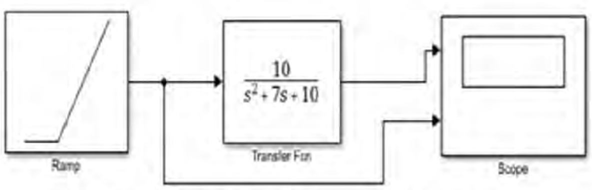

Fig. 18 SIMULINK Block Diagram of Ramp input

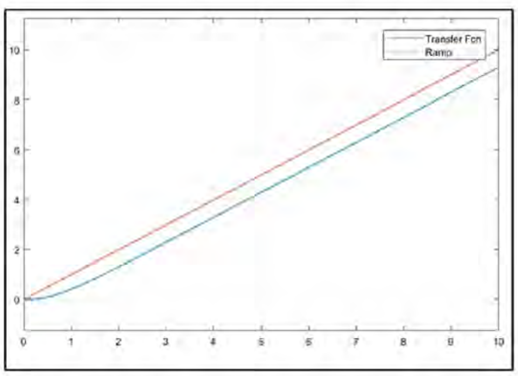

Fig 19. Response Plot of system against a Ramp Input

The response is lacking behind the input command hence causing steady state error.

B. Stability of System

From all the above plots, we concluded that our system is stable and only a few alternations are required (which will be done by implementing either of the P, PD or PID controller) to make it suitable for our application. Such as we can control the settling time and overshoot etc.

The open loop transfer function with P controller K and unity feedback system, in a block diagram is:

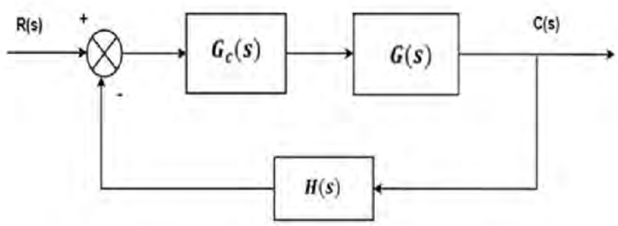

Fig. 20 Block Diagram of closed-loop function of system proportional controller G_c

For the intended system, a P-controller is implemented with a unity feedback system.

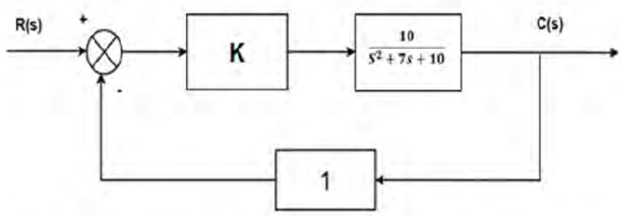

Fig. 21 Block Diagram of system having gain K and unity feedback.

The following system can be reduced to get equivalent transfer function T(s).

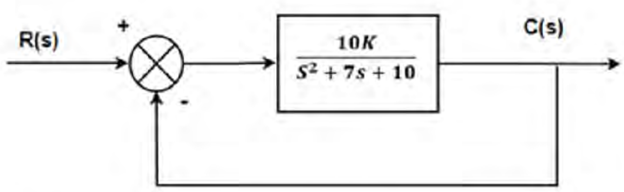

Fig. 22 Simplified closed-loop transfer function with unity feedback.

As we know that:

$$T(s) = \frac{G(s)}{1 + G(s)H(s)}$$

By putting values of G(s) we get closed loop transfer function as:

$$T(s) = \frac{10K}{s^2 + 7s + 10(K + 1)} \quad [20]$$

With the help of Routh Hurwitz technique, we can find the whether the system is stable or not and for which range of P-controller gain K it is stable. Making Routh table with initial assumption that K>0:

TABLE. 2 ROUTH HURWITZ TABLE

s^2	1	10(K+1)	0
s^1	7	0	0
s^0	10(k+1)	0	0

- For a stable system:

k>-1

- For the system to be marginally stable:

k=-1

- For the system to be unstable:

k<-1

Since in the beginning we made assumption that *K>0* therefore our P-controller gain K varies from 0 to *+∞ or k>-1.*

C. Steady State Errors of the System for different inputs

$$E(s) = \frac{R(s)}{1 + G(s)}$$

Applying final value theorem, we get,

$$e(\infty) = \lim_{s\to 0} \frac{sR(s)}{1 + G(s)} \quad [21]$$

For Step Input:

$$R(s) = \frac{1}{s}$$

$$e(\infty)_{step} = \frac{1}{1 + K_p} = \frac{1}{1 + \lim_{s\to 0} G(s)}$$

$$G(s) = \frac{10}{s^2 + 7s + 10}$$

$$e(\infty)_{step} = \frac{1}{1 + \lim_{s\to 0} \left(\frac{10}{s^2 + 7s + 10}\right)}$$

$$e(\infty)_{step} = \frac{1}{2}$$

For Ramp Input:

$$R(s) = \frac{1}{s^2}$$

$$e(\infty)_{step} = \frac{1}{K_v} = \frac{1}{1 + \lim_{s\to 0} sG(s)} \quad [22]$$

$$e(\infty)_{ramp} = \frac{1}{\lim_{s\to 0} s(s^2 + 7s + 10)}$$

$$e(\infty)_{ramp} = \infty$$

For Parabolic Input:

$$R(s) = \frac{1}{s^3}$$

$$e(\infty)_{parabolic} = \frac{1}{K} = \frac{1}{\lim s^2 G(s)} \quad [23]$$

$$e(\infty)parabolic = \infty$$

We can conclude from this that our system is Type 0 system where for step input error is ½ while for ramp and parabolic input steady state error is infinite.

D. Plotting Root Locus

Finally plotting the root locus using MATLAB. Root Locus is a influential method of examination and design for stability and transient response.

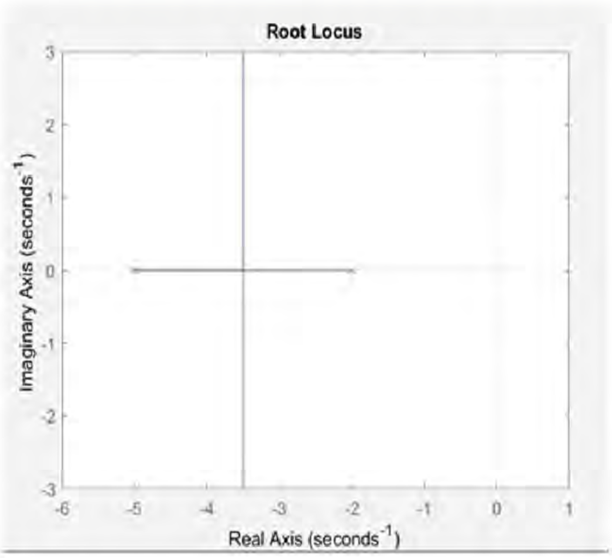

Fig. 23 Root-Locus plot of Function for different values of gain k.

From the plot, we conclude that root locus poles of our system are on real axis no pole is on imaginary axis. The asymptotes of system go to infinity Note: This is the plot of the system itself with no controller.

VII. Controller Design

By plotting the response of the system against step input, it is observed that an error of 0.50 is appearing and for ramp and parabolic inputs the errors appear to be infinity because the system is type 0 system and, in that case, k_v and k_a are 0 making the errors infinity. Moreover, a settling time of 2.211 sec is observed, both these characteristics were not desirable under the situation and were meant to be improved. Less settling time and faster response along with least possible steady-state error was the requirement of the situation. Since the system response is ''Over-damped'' corresponding to ζ=1.10 (which is > 1). The only issue with the system appears to be steady state-error along with settling time and transient response to be quick. These characteristics were tried to be improved by usage of PID controller. The usage of PID-controller proved to be useful and gave the response that was required. MATLAB PID-Tuner was used to find the required values for gains of P, I and D controllers and then the values of k_p and k_i and k_d were altered until the required response was achieved. The improved system response is as follow:

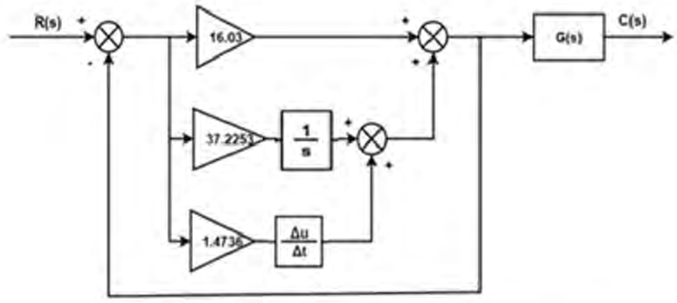

Fig. 24 Block Diagram of system having PID Controller

The values of the proportional, derivative, and integrator gains were tuned to get the desired response. After playing around with the values a bit, we settled on the following combination.

TABLE 3. PID Controller Parameters for the Stable System

Controller Parameters	
P	16.0328
I	37.2253
D	1.4736
N	1811.2603

According to these parameters the controller gives us the following plot.

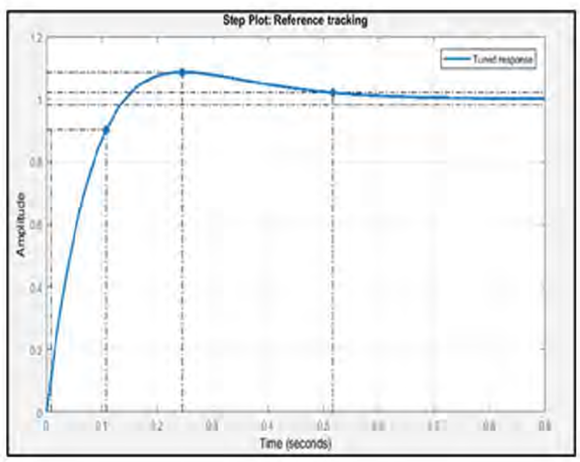

Fig. 25 Improved Response Of system after PID implementation

The tuned response has no steady-state error along with the desired % overshoot and settling time. System has stable response with improved characteristics.

Performance and Robustness

	Tuned
Rise time	0.1 seconds
Settling time	0.517 seconds
Overshoot	8.56 %
Peak	1.09
Gain margin	Inf dB @ Inf rad/s
Phase margin	77 deg @ 15.8 rad/s
Closed-loop stability	Stable

Fig. 26 Improved characteristics of system with PID

Comparison of Improved and original parameters results is given:

TABLE 4. COMPARISONS OF IMPROVED AND UN-IMPROVED PARAMETERS

Parameters	Un-improved	Improved
Steady-state error	0.5	0
Settling time	2.2112 sec	0.517 sec
Overshoot	0 %	8.56 % (desired)
Rise time	1.232 sec	0.11 sec

After the successful implementation of PID in our system we see that the system response has been improved and system is achieving the steady state with decreased rise time and decreased settling time. But system has an overshoot 8.5% which is not a problem for system response. The fundamental weakness of this study is that the initial values of the transfer function were set with the presumption that they would immediately provide us a stable transfer function.

VIII. CONCLUSIONS

In a power generation plant, a balance between load requirements and power generation value is very important for the controlled and smooth working of all interconnected generating units. In actuality, a single generator usually supplies a broad region. A geographical area's power demands will be met by several parallel generators positioned in different locations. All of these generators should have the same response characteristics to variations in load demand. The disturbances caused by the load frequency changes have to rejected and to maintain a constant value for synchronization of generators. Changes in frequency can cause power converters to malfunction by generating harmonics. When operating at frequencies lower than 49.5 Hz, some rotor states in specific types of steam turbines experience significant vibration. These vibrations are not desirable and can decreases efficiency as well the life of steam turbine. Many adaptive studies and experiments based on the different intelligent techniques have been implemented to solve the issues. However, these solutions need either system state information or an efficient online identification. The model reference technique may be challenging to implement due to the high order model of system. To have better and simple solution we have used the exact controller transfer function modelled from the quotative feedback theory (QFT) and tested it again different input commands to see the system response. We have designed a PID controller to get the desirable characteristics of system. Simulations of system are done by using MATLAB and Simulink. PID tuner is used to get the desired PID parameters and we have performed many iterations of tuning parameters at different values of k_p and k_i and k_d. After these so many iterations we get the required values of PID parameters on which our system shows the behaviour which is according to the requirement of situation. Results of MATLAB simulations and PID-tuner shows that the suggested PID works better than the conventional PI controller in terms of dampening the power system after a step change in load.

IX. FUTURE RECOMENDATIONS

This work is based on the QFT based modelled control system and is limited for single area load frequency control. It can be extended to multi-area load frequency control of power system for a number of applications in future.

REFERENCES

[1] S. Sönmez and S. Ayasun, "Stability Region in the Parameter Space of PI Controller for a Single-Area Load Frequency Control System With Time Delay," *IEEE Trans. Power Syst.*, vol. 31, no. 1, pp. 829–830, 2016, doi: 10.1109/TPWRS.2015.2412678.

[2] K. Jung, J. Park, Y. Moon, and H. Rhew, "Extended Integral Control for Load Frequency Control With the Consideration of Generation-Rate Constraints," no. C, pp. 1–6, 2000.

[3] H. S. Ryu, K. Il Min, J. G. Lee, and Y. H. Moon, "Extended integral based governor control for power system stabilization," *Proc. IEEE Power Eng. Soc. Transm. Distrib. Conf.*, vol. 3, no. SUMMER, pp. 1610–1614, 2002, doi: 10.1109/pess.2002.1043662.

[4] A. Khodabakhshian and N. Golbon, "UNIIFIED PID DESIGN FOR LOAD FREQUENCY CONTROL."

[5] A. Khodabakhshian and N. Golbon, "Design of a new load frequency PID controller using QFT," *Proc. 20th IEEE Int. Symp. Intell. Control. ISIC '05 13th Mediterr. Conf. Control Autom. MED '05*, vol. 2005, pp. 970–975, 2005, doi: 10.1109/.2005.1467145.

[6] Y.-H. M.-S. Ryu, B. Kim, S. Kim, and S.-C. Park, "Fuzzy Logic Based Extended Integral Control for Load Frequency Control," 2000.

[7] M. I. Mosaad and F. Salem, "LFC based adaptive PID controller using ANN and ANFIS techniques," *J. Electr. Syst. Inf. Technol.*, vol. 1, no. 3, pp. 212–222, Dec. 2014, doi: 10.1016/j.jesit.2014.12.004.

[8] W. Tan and Z. Xu, "Robust analysis and design of load frequency controller for power systems," *Electr. Power Syst. Res.*, vol. 79, no. 5, pp. 846–853, May 2009, doi: 10.1016/j.epsr.2008.11.005.

[9] D. G. Padhan and S. Majhi, "A new control scheme for PID load frequency controller of single-area and multi-area power systems," *ISA Trans.*, vol. 52, no. 2, pp. 242–251, 2013, doi: 10.1016/j.isatra.2012.10.003.

[10] N. Anwar and S. Pan, "Electrical Power and Energy Systems A new PID load frequency controller design method in frequency domain through direct synthesis approach," *Int. J. Electr. POWER ENERGY Syst.*, vol. 67, pp. 560–569, 2015, doi: 10.1016/j.ijepes.2014.12.024.

[11] S. Sondhi and Y. V. Hote, v"Fractional order PID controller for perturbed load frequency control using Kharitonov's theorem," *Int. J. Electr. Power Energy Syst.*, vol. 78, pp. 884–896, Jun. 2016, doi: 10.1016/j.ijepes.2015.11.103.

[12] W. Tan, "Unified tuning of PID load frequency controller for power systems via IMC," *IEEE Trans. Power Syst.*, vol. 25, no. 1, pp. 341–350, Feb. 2010, doi: 10.1109/TPWRS.2009.2036463.

[13] K. Sabahi, A. Hajizadeh, M. Tavan, and A. Feliachi, "Adaptive Type-2 Fuzzy PID LFC for an Interconnected Power System Considering Input Time-Delay," *Int. J. Fuzzy Syst.*, vol. 23, no. 4, pp. 1042–1054, Jun. 2021, doi: 10.1007/s40815-020-01017-2.

[14] S. Duman, N. Yorukeren, and I. H. Altas, "Load frequency control of a single area power system using gravitational search algorithm," *INISTA 2012 - Int. Symp. Innov. Intell. Syst. Appl.*, vol. 9, no. 05, pp. 1318–1320, 2012, doi: 10.1109/INISTA.2012.6246992.

[15] T. Anitha, G. Gopu, M. Nagarajapandian, and P. A. M. Devan, "Hybrid Fuzzy PID Controller for Pressure Process Control Application," 2019 *IEEE Student Conf. Res. Dev. SCOReD 2019*, pp. 129–133, 2019, doi: 10.1109/-SCORED.2019.8896276.

[16] M. R. Toulabi, M. Shiroei, and A. M. Ranjbar, "Robust analysis and design of power system load frequency control using the Kharitonov's theorem," *Int. J. Electr. Power Energy Syst.*, vol. 55, pp. 51–58, 2014, doi: 10.1016/j.ijepes.2013.08.014.

[17] P. Sonkar and O. P. Rahi, "Integrated tuning of PID-derivative load frequency controller for two area interconnected system via IMC," *2015 2nd Int. Conf. Recent Adv. Eng. Comput. Sci. RAECS 2015*, vol. 7, no. 3, pp. 42–51, 2016, doi: 10.1109/RAECS.2015.7453417.

[18] S. Hanwate, Y. V. Hote, and S. Saxena, "Adaptive policy for load frequency control," *IEEE Trans. Power Syst.*, vol. 33, no. 1, pp. 1142–1144, 2018, doi: 10.1109/TPWRS.2017.2755468.

[19] S. Jain and Y. V. Hote, "Generalized Active Disturbance Rejection Controller for Load Frequency Control in Power Systems," *IEEE Control Syst. Lett.*, vol. 4, no. 1, pp. 73–78, 2020, doi: 10.1109/LCSYS.2019.2923168.

[20] S. Saxena, "Electrical Power and Energy Systems Load frequency control strategy via fractional-order controller and reduced- order modeling," *Electr. Power Energy Syst.*, vol. 104, no. May 2018, pp. 603–614, 2019, doi: 10.1016/j.ijepes.2018.07.005.

[21] S. Debbarma, L. Chandra, and N. Sinha, "Electrical Power and Energy Systems Automatic generation control using two degree of freedom fractional order PID controller," *Int. J. Electr. Power Energy Syst.*, vol. 58, pp. 120–129, 2014, doi: 10.1016/j.ijepes.2014.01.011.

[22] Y. Arya, "A new optimized fuzzy FOPI-FOPD controller for automatic generation control of electric power systems," *J. Franklin Inst., 2019,* doi: 10.1016/j.jfranklin.2019.02.034.

[23] D. K. Gupta, A. V. Jha, B. Appasani, A. Srinivasulu, N. Bizon, and P. Thounthong, "Load frequency control using hybrid intelligent optimization technique for multi-source power systems," *Energies,* vol. 14, no. 6, 2021, doi: 10.3390/en14061581.

[24] M. Gheisarnejad and M. H. Khooban, "Secondary load frequency control for multi-microgrids: HiL real-time simulation," *Soft Comput.,* vol. 23, no. 14, pp. 5785–5798, 2019, doi: 10.1007/s00500-018-3243-5.

[25] A. Annamraju and S. Nandiraju, "Frequency Control in an Autonomous Two-area Hybrid Microgrid using Grasshopper Optimization based Robust PID Controller," *India Int. Conf. Power Electron. IICPE,* vol. 2018-Decem, pp. 1–6, 2018, doi: 10.1109/IICPE.2018.8709428.

[26] Y. Arya, "Automatic generation control of two-area electrical power systems via optimal fuzzy classical controller," *J. Franklin Inst.,* vol. 355, no. 5, pp. 2662–2688, 2018, doi: 10.1016/j.jfranklin.2018.02.004.

[27] M. Gheisarnejad and M. H. Khooban, "Design an optimal fuzzy fractional proportional integral derivative controller with derivative filter for load frequency control in power systems," *Trans. Inst. Meas. Control,* vol. 41, no. 9, pp. 2563–2581, 2019, doi: 10.1177/0142331218804309.

[28] M. A. Magzoub and T. Alquthami, "Optimal Design of Automatic Generation Control Based on Simulated Annealing in Interconnected Two-Area Power System Using Hybrid PID—Fuzzy Control," *Energies,* vol. 15, no. 4, 2022, doi: 10.3390/en15041540.

[29] D. Sambariya and V. Nath, "Load Frequency Control Using Fuzzy Logic Based Controller for Multi-area Power System," *Br. J. Math. Comput. Sci.,* vol. 13, no. 5, pp. 1–19, 2016, doi: 10.9734/bjmcs/2016/22899.

[30] D. K. Sambariya and R. Prasad, "Optimal Tuning of Fuzzy Logic Power System Stabilizer Using Harmony Search Algorithm," *Int. J. Fuzzy Syst.,* vol. 17, no. 3, pp. 457–470, 2015, doi: 10.1007/s40815-015-0041-4.

Dynamic Traffic Control and Management System Utilizing Real-Time Image Processing: A Sustainable Approach for Traffic Congestion in Developing Countries

M Atif Saeed
Mechatronics Dept.
Shaheed Zulfiqar Ali Bhutto Institute of Science and Technology
m.atif@szabist.edu.pk

Abstract -- Traffic congestion and management pose critical challenges in urban cities and developing countries, particularly in South Asian countries like Pakistan. The problem has escalated due to the exponential growth in the number of vehicles and inadequate road infrastructure. This issue goes beyond mere traffic congestion, as it is accompanied by air pollution, wastage of valuable resources such as fuel, energy, and time, and has adverse effects on the overall well-being of individuals in third world countries. Furthermore, it contributes to global warming and disrupts natural ecosystems. The current traffic control system in Pakistan relies mainly on time-based traffic signal systems. In this study, we propose a dynamic traffic control and management system that utilizes real-time image processing to make informed decisions regarding traffic routes and signal timings. By harnessing the latest advancements in image processing technology, our system collects, organizes, and transmits data to the existing traffic control infrastructure, enabling the integration of up-to-date information for efficient traffic timing control. This system aims to improve road safety, reduce accidents, and minimize unnecessary fuel consumption, ultimately enhancing the quality of life for individuals. By implementing this innovative approach, we anticipate significant improvements in traffic flow, reduced congestion, and optimized resource utilization. The utilization of real-time data and intelligent decision-making based on image processing technologies offers a promising solution to address the pressing issues associated with traffic control in Pakistan. This research contributes to the development of a more sustainable and efficient traffic management system, benefiting both individuals and the environment.

Keywords -- traffic control, traffic management, developing countries, traffic congestion, image processing, real-time, road infrastructure, air pollution, resource wastage, fuel efficiency, sustainability.

1. Introduction

In contemporary times, numerous investigations have delved into the ramifications of technology on human existence, constitution, and self-identity [1]–[4]. These studies consistently propose that humans have historically harnessed diverse technological instruments and objects to mold themselves. For instance, consider the MRI scan or microscope, which have evolved into indispensable tools for medical inquiries and diagnoses [5]–[9]. Medical interventions, medications, and even dietary schemas are formulated based on outcomes and analyses derived from these technological innovations. This underscores the substantial impact of technology on the human condition. These advancements not only enhance human life by offering convenience and comfort but also imbue an essence of opulence [10]–[13]. Nevertheless, despite this modernization, specific domains of human life remain relatively underexplored in terms of research, which could address ongoing challenges.

In a world populated by over 8 billion individuals [14] and accommodating 1.2 billion automobiles on the streets [15], traffic congestion has evolved into a daily ritual for many. Regardless of geographical location, billions of people encounter the exasperation of traffic gridlock, leading to squandered time and fuel. A critical breakthrough in the transportation realm is urgently required to rectify this concern and enrich the quality of human existence. As reported in a Forbes article, traffic congestion solely in the United States resulted in a $124 billion economic deficit in 2013, with projections estimating an escalation to $186 billion by 2030 [16]–[20]. The INRIX report further anticipates a worsening traffic scenario by 2030, given the prevailing pace of population expansion [21]. Acknowledging the significance of tackling traffic congestion, the United Nations has included it as a target within the broader global UN objectives for 2030 [22], *aiming to "Ensure access to affordable, reliable, sustainable, and modern transportation for all, improving road safety, particularly by expanding public transport, focusing on the needs of marginalized individuals, women, children, people with disabilities, and senior citizens."*

Addressing this worldwide challenge mandates substantial endeavors. Several theoretical frameworks have emerged as potential remedies, encompassing:

- Adaptive traffic signal systems
- Autonomous vehicular technology
- Substituting vehicles with drones

Among these alternatives, adaptive traffic signals currently emerge as the most viable choice [23]–[27]. These systems have the potential to substantially alleviate the global traffic predicament while minimizing the necessity for extensive alterations to existing infrastructure. The present paper is dedicated to the formulation and execution of an adaptive traffic signal system within the context of 3talwar, Karachi.

A. Adaptive Traffic Signal

The existing traffic signal installations presently function on a predetermined timetable that orchestrates signal changes utilizing collected data. This data is garnered by observing signal behavior across a designated timeframe, identifying periods of peak activity, lulls, and instances of moderate traffic. Lane-specific data is also factored in, allowing for manual timing adjustments for individual lanes, which are then input into the pre-established system. However, this pre-arranged approach fails to accommodate situations like holidays, Election Day, or labor strikes. In contrast, the adaptive traffic signal technology possesses the capacity to adapt red, green, and yellow light durations based on real-time traffic dynamics. This technological progression holds the promise of endowing the system with autonomous decision-making capabilities, consequently mitigating traffic congestion. The pivotal merits of adaptive traffic signals, when juxtaposed with conventional counterparts, encompass:

- Improving traffic flow
- Swift adaptation to prevailing traffic conditions
- Reduction in operational expenses

a) Enhancement of traffic stream

One of the persisting issues with the existing traffic signal systems is the common occurrence of drivers being held up at red lights, even when the lane is clear. Conversely, there are instances where a lane becomes overly congested, yet the traffic signal switches to green, forcing drivers to move forward only to become stuck shortly after. The goal is to elevate the functionality of these signals by imbuing them with intelligence that enables adaptation to real-time conditions and the ability to make well-informed decisions [28].

a) Enhancement of traffic stream

One of the persisting issues with the existing traffic signal systems is the common occurrence of drivers being held up at red lights, even when the lane is clear. Conversely, there are instances where a lane becomes overly congested, yet the traffic signal switches to green, forcing drivers to move forward only to become stuck shortly after. The goal is to elevate the functionality of these signals by imbuing them with intelligence that enables adaptation to real-time conditions and the ability to make well-informed decisions [28].

The envisaged technology offers a viable solution to this challenge. The system is comprised of strategically positioned sensors that continuously gather real-time data, which is then relayed to a processor for meticulous analysis and decision-making. These sensors could take the form of well-placed cameras, capturing ongoing lane images and transmitting them to the processor. Employing a range of advanced image processing techniques, the processor evaluates the images against predefined criteria, thereby enabling proactive decision-making. This innovation holds immense potential to enhance the driving experience for both local and international commuters on roadways and highways alike. By curtailing avoidable delays, traffic flow gains momentum and becomes more fluid.

b) Swift adaptation to prevailing traffic conditions

At present, signal timing, adjustments hinge on manually collected data, a rigid approach that lacks the agility to respond to unforeseeable traffic fluctuations. This rigidity often leaves drivers ensnared in traffic snarls, resulting in grievances and compromising safety. These complaints serve as the basis for officials to fine-tune signal timings. However, when no complaints are registered, citizens might have to endure extended spells of inconvenience. In stark contrast, adaptive signals possess the capability to dynamically address these variables in real-time, flexibly altering their timing based on a sophisticated algorithmic approach [29].

c) Reduction in operational expenses

Research conducted by the Texas Transportation Institute underscores that traffic congestion incurs an annual loss of approximately $87.2 billion due to fuel consumption and reduced productivity. This translates to an average cost of $750 per individual [30]. The existing traffic signal infrastructure places a substantial financial burden on businesses and individuals alike. These signals are responsible for over 10% of all traffic delays, consequently amplifying fuel usage and curtailing business efficiency. By ushering in adaptive signal control mechanisms, these financial strains can be significantly alleviated through intelligent and automated adjustments grounded in updated data streams. Crucially, signal-timing adaptations correspond to real-time traffic dynamics, extending tangible benefits to citizens.

II. Comparison with Existing Techniques

A. Existing Traffic Control Systems

The paper identifies that the current traffic control system in Pakistan relies mainly on time-based traffic signal systems. These systems operate on a pre-programmed schedule, switching lights according to collected data. While manual adjustments can be made based on historical data, they lack the flexibility to adapt to real-time traffic conditions, leading to inefficiencies and congestion during unexpected events or variations in traffic patterns.

B. Adaptive Traffic Signal Systems

The proposed system introduces adaptive traffic signals that utilize real-time image processing technology to make informed decisions regarding traffic routes and signal timings. Adaptive traffic signals have been explored in the past as potential solutions to address traffic congestion. They have the potential to improve traffic flow, respond faster to changing traffic conditions, and cut costs associated with congestion. However, the paper highlights that existing adaptive traffic signal systems often rely on transducers like IR or strain gauges to detect vehicles, which might be limited in accuracy and require additional infrastructure.

C. Novelty of the Proposed System

The proposed system's novelty lies in its utilization of real-time image processing techniques, specifically the implementation of Otsu's Thresholding Approach, to address traffic congestion. By employing cameras installed at traffic signal poles, the system captures wide-angle images, processes them using image processing algorithms, and then makes decisions based on predetermined criteria. This approach removes the need for additional transducers and provides a cost-effective solution to implement an adaptive traffic control system.

The paper's proposed system stands out for the following reasons:

- Real-Time Image Processing: The system's reliance on real-time image processing technology sets it apart from conventional traffic control systems. This allows the system to dynamically adjust signal timings based on actual traffic conditions, making it more responsive and efficient.
- Cost-Effectiveness: The proposed system requires minimal additional hardware since it leverages existing traffic signal poles and night vision cameras. This cost-effective approach makes it feasible for implementation in resource-constrained environments.
- Intelligent Decision-Making: By using Otsu's Thresholding Approach, the system can accurately identify traffic density levels and adjust signal timings accordingly. This intelligent decision-making contributes to reducing congestion and optimizing traffic flow.
- Flexibility and Adaptability: The system is designed to handle various traffic scenarios, such as medium to high traffic density, traffic congestion from all directions, and even scenarios with limited visual data (e.g., complete darkness). This flexibility ensures effective traffic management under diverse conditions.
- Sustainability: By improving traffic flow and reducing congestion, the proposed system contributes to sustainability efforts by minimizing fuel consumption and emissions, leading to a positive impact on the environment.

III. System Integration and methodology

This research introduces an integrated solution that leverages digital image processing techniques to tackle the global issue of traffic congestion. Unlike prevalent adaptive traffic signal systems that rely on transducers such as infrared (IR) or strain gauges for vehicle detection, this innovative approach incorporates cameras positioned at an elevation of 8-10 meters alongside traffic signal poles. These cameras capture wide-angle images, forming the foundation for implementing appropriate algorithms.

Given the extensive pixel count in raw images, these pixels will undergo a systematic process guided by predefined criteria to yield desired outcomes. To facilitate this, a reference image of an unoccupied road will be provided by the user. Subsequently, each captured image will be juxtaposed with the reference image, and a comparative analysis will be conducted based on their respective grayscale levels.

The captured images will be partitioned into three distinct zones: low, medium, and high. These zones will be determined using a density function that assesses the number of gray pixels in each image and contrasts it with the reference image. Furthermore, explicit scenarios have been established to regulate the timing of red, yellow, and green lights contingent upon the detected zone. The intricate workflow of this system is depicted in Figure 1 below.

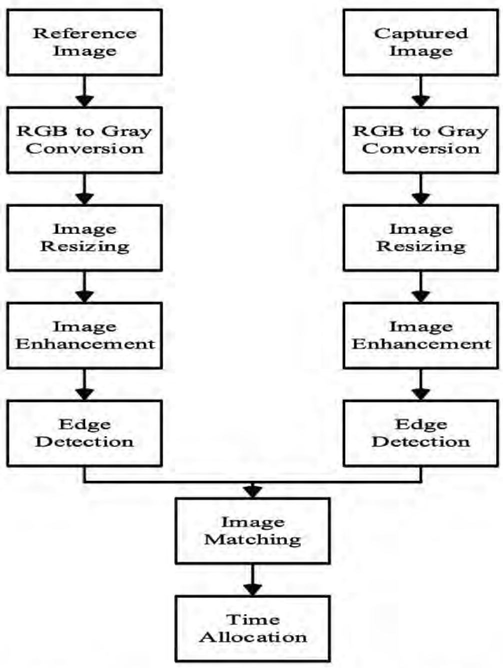

Figure 1: System description of traffic signal algorithm

The central objective of this proposed research is to amplify the effectiveness of the existing system by introducing an automated traffic light mechanism rooted in traffic density analysis. Notably, this innovative approach exclusively hinges on image processing methodologies. It is pertinent to note that this system's blueprint has been tailored for implementation at the 3talwar signal in Karachi. Renowned as one of the city's most bustling intersections, this signal grapples with a daily vehicular influx ranging from 40,000 to 50,000 cars. Such substantial traffic numbers paint a vivid picture of the challenges encountered during peak hours. The signal's representation during high traffic is depicted in Figure 2, while the absence of vehicles on quieter days is illustrated in Figure 3. The labeled road diagram, integral for the mapping process, is showcased in Figure 4.

Figure 2: 3 talwar, busy day

Figure 3: 3talwar, slow day

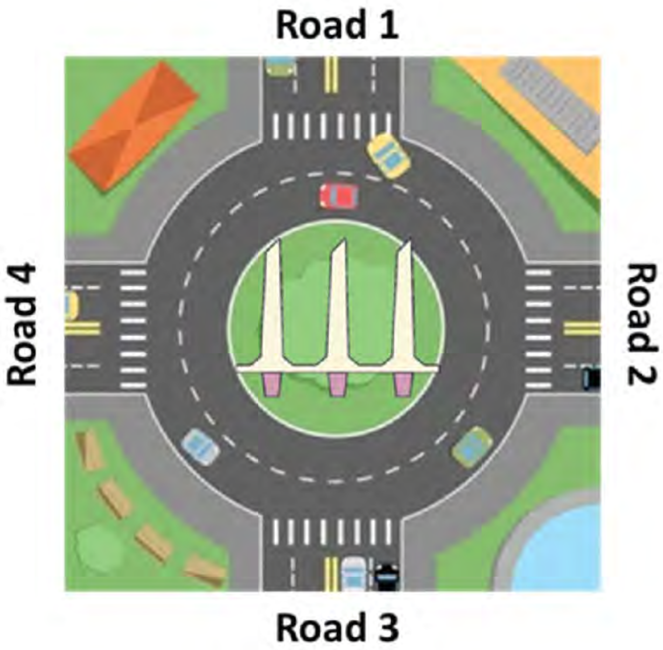

Figure 4. Road Label

The traffic signal framework adheres to a predetermined chronological sequence, where each facet of the signal is initially allocated 10 seconds for the green light, succeeded by 5 seconds for the yellow light, and culminating with 60 seconds for the red light. The signal's progression consistently follows a clockwise trajectory. Positioned atop an iron rod standing at an approximate height of 8-10 meters, each traffic signal is accompanied by a state-of-the-art night vision camera. The vicinity encircling the signal is segmented into three distinct categories, delineated by distance: the range of 21-40 feet signifies low vehicle density, 41-60 feet embodies medium vehicle density, while 61-90 feet designates high vehicle density. The underlying algorithm has been meticulously crafted to navigate through diverse scenarios contingent upon these density-based divisions.

In the first scenario, if the vehicle density registers at a medium level or below, the signal will illuminate the green light for a duration of 10 seconds before promptly transitioning to red. Given the clockwise sequential shift of signals, this pattern seamlessly perpetuates for the ensuing signal in the circuit.

Alternatively, in the second scenario, as vehicles persistently ingress into the high-density precinct, the system will capture an image within the initial five seconds of the green light cycle. This image will be expedited to the microprocessor for comprehensive analysis. Guided by the algorithm's dictates, the microcontroller will recali- brate the signal's temporal intervals, resetting them from 2 to 12 seconds or from 0 to 10 seconds. This adjustment can be executed a maximum of twice in the event of persistent identical circumstances; contrarily, the signal will revert to its original temporal configuration, progressing to the subsequent signal node.

In the third scenario of high traffic density on all four sides of the road, the traffic control system faces a challenging situation with heavy congestion from all directions. To handle this efficiently, the system continuously monitors traffic density using real-time image processing and employs a dynamic traffic signal adjustment strategy. It prioritizes green signal time for the busiest lanes to allow them to clear quickly, while also distributing green time based on detected traffic density to ensure fairness. Traffic preemption techniques may be used to prioritize emergency vehicles or public transportation, creating gaps for smoother merging. Temporary lane reconfigurations can further optimize traffic flow. With efficient algorithms, parallel processing, and hardware acceleration, the system adapts to changing traffic conditions, efficiently managing high-density traffic without compromising performance.

In the fourth scenario of complete darkness, the traffic control system faces the challenge of lacking visual data from image processing. To overcome this, the system relies on alternative sensors like infrared or radar to detect vehicle presence and movement. Using adaptive algorithms and predictive models, it adjusts traffic signal timings based on the sensor data and historical information. Safety measures are prioritized with longer yellow signals and extended green signals on major roads to ensure smoother traffic flow and minimize potential collisions. Although visual data is valuable, the system's ability to adapt using alternative sensors and predictive models ensures functional and safe traffic control even in the absence of visual information.

The envisaged system's programming will be exclusively carried out within the MATLAB environment to facilitate modeling and simulation. Departing from the application of Global Thresholding, our methodology will embrace the utilization of Otsu's Thresholding Approach. The conventional Global Thresholding approach proves less tenable when confronted with uneven illumination across the image, thereby leading to discernible variations in brightness and darkness within distinct sections. On the contrary, Otsu's Thresholding method offers a more apt alternative for our specific investigation, given the coexistence of dynamic and stationary elements [31]. Notably, Otsu's Thresholding adeptly surmounts challenges encompassing pronounced illumination gradients, disparities in grey levels between foreground and background, as well as limited contrast.

By segmenting the grey level histogram into two discernible clusters, Otsu's method systematically identifies the threshold that maximizes variance between these distinct groups. This strategic approach proves resilient in generating satisfactory outcomes even in scenarios where the grey level image histogram fails to manifest two distinctly pronounced peaks. The intricate operations underpinning Otsu's algorithm are graphically illustrated in Figure 5.

$$PDF_{Gaussian} = \frac{1}{\sqrt{2\pi}\sigma} e^{\frac{(g-\mu)^2}{2\sigma^2}}$$

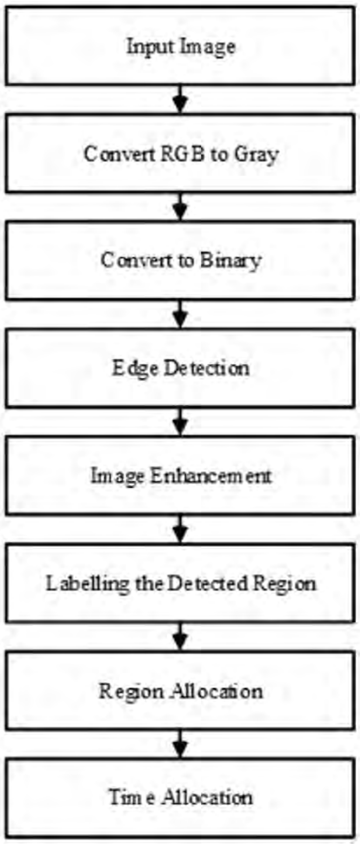

Figure 5: Otsu's Algorithm

1. Initiate the process by ascertaining the uppermost and lowermost extents of grey levels prevalent within the image.
2. Designate the minimum value as the inaugural threshold (To) for reference. Grounded in this threshold, delineate the pixel values constituting the image into two distinct clusters: Co, representing the set of grey level values less than or equal to the initial threshold, and C1, encapsulating pixel values with grey levels surpassing the initial threshold.
3. Let N and A stand respectively for the count of pixels and the average grey level value pertaining to groups Co and C1. The mean grey level value for all pixels can then be determined using Equation 2.

$$M_T = \frac{N_o \mu_o + N_1 \mu_2}{N_o + N_1}$$

4. Subsequently, the computation of variance for the two pixel groups becomes imperative. Variance serves as a metric denoting the degree of dispersion within data sets, characterizing their mean grey level values or images. The variance computation is accomplished through Equation 3.

$$\alpha^2(T_O) = \{ N_O (\mu_o - M_T)^2 + N_1(\mu_1 - M_T)^2\}$$

5. Concluding the process, the task of discerning the threshold value aligning with the highest variance materializes. The integration of Otsu's algorithm into our system's framework is vividly portrayed in Figure 6 below.

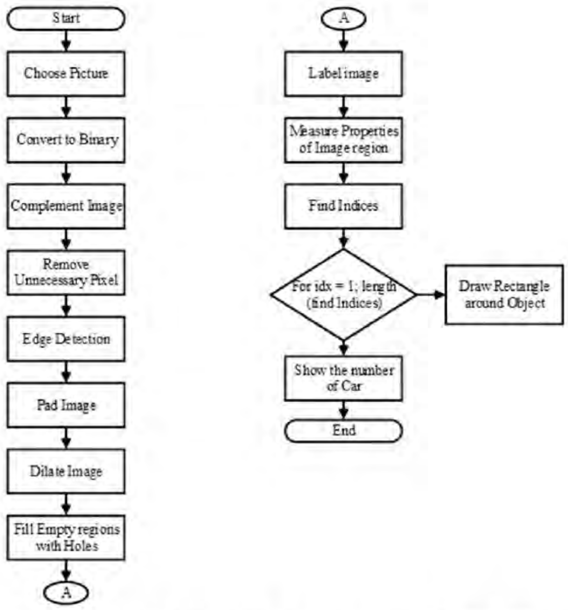

Figure 6: Otsu's Algorithm implemented on our system

IV. Analysis and Results

This segment offers a comprehensive scrutiny of the system as governed by the stipulated algorithm. Each sequential action outlined in the algorithm will be expounded upon, accompanied by relevant illustrative images. As previously emphasized, the provision of a reference image portraying an unoccupied road holds paramount significance for facilitating pixel density comparison. This underpins the categorization of distinct regions, namely low, medium, and high densities. The visual representation of the system's reference image is depicted in Figure 7 below.

Figure 7: Reference image

For the ensuing analysis, one representative image has been chosen, featured in Figure 8.

Figure 8: Input image

The initial step of the process involves converting the input image into grayscale, a pivotal step that streamlines pixel density assessment. Subsequently, the grayscale depiction is juxtaposed with the reference image, undergoing inversion according to our tailored algorithm, as visually depicted in Figure 9. To execute this operation, the Canny operator, renowned for its edge detection capabilities, is harnessed to segment real-time images. Edges, lines, and points are salient features within an image, and in this research, we harness edge detection on the grayscale image to delineate edges and establish delineations amid varying regions. The core objective is to synchronize the edges present in real-time images with those of the reference image, thereby discerning the extent of concurrence and subsequently categorizing traffic density levels into low, medium, and high. This critical intelligence steers the controller in determining optimal timing configurations for traffic signals. Given the inapplicability of thresholding-based segmentation due to the presence of vehicles characterized by varying colors that defy effective thresholding, the application of edge detection becomes the apt approach for image alignment. This alignment process involves correlating a reference image with a real-time acquired image and subsequently assessing the alignment of their respective edges. This alignment percentage serves as the bedrock for ascertaining traffic density levels. Subsequent to this analysis, the controller iterates upon the traffic signal timing settings.

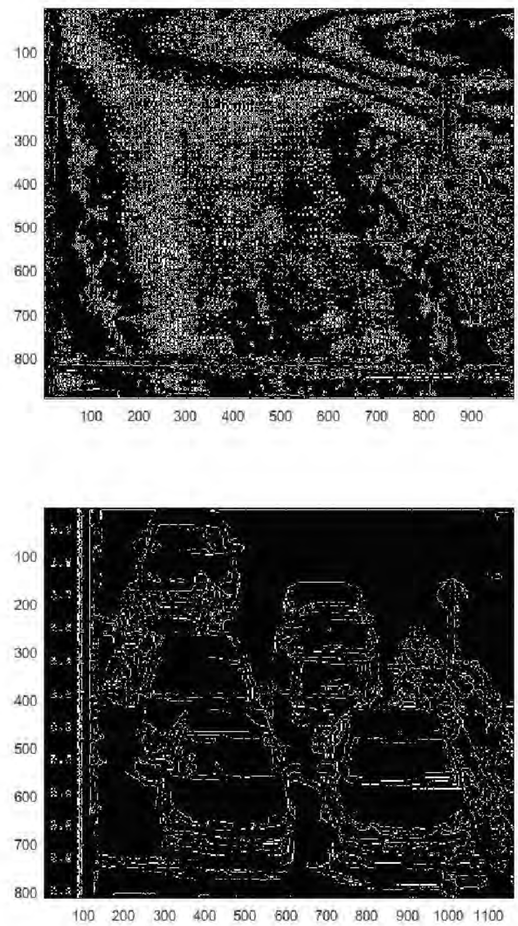

Figure 9: Output image

The algorithm proceeds by quantifying the count of white and black pixels, utilizing equations 1, 2, and 3 to definitively establish the regions indicative of traffic density. A comprehensive operation demonstration for the signal is furnished in Table 1.

Table 1: Demo working of signal

Camera	Road 1	Road 2	Raod 3	Road 4	Duration
Innitial Capture	Red	Red	Red	Red	10
Start with high density	Green	Red	Red	Red	20
	Yellow	Yellow	Red	Red	4
Low density	Red	Green	Red	Red	10
		Yellow	Yellow		4
Low density	Red	Red	Green	Red	10
	Red	Red	Yellow	Yellow	4
High density	Red	Red	Red	Green	20
Emergency at Road 3	Red	Red	Yellow	Yellow	4
	Red	Red	Green	Red	till emergency
Emergency cleared	Yellow		Yellow		4
Normal	Green	Red	Red	Red	10

Table *1* effectively showcases the functionality of the proposed traffic signal algorithm across diverse scenarios. Let's delve into the explication of each step:

- Initialization: Commencing from a baseline, all four traffic signals initiate at zero, symbolizing the red signal status for all lanes.
- Detection of High-Intensity Zone: The instant the system discerns the initial high-intensity zone, denoting substantial traffic within a specific lane, the signal for said lane transitions to green for a duration of 20 seconds. Throughout this interval, the three remaining lanes remain designated as red.
- Identification of a Second High-Intensity Zone: Concurrently, within the 16-second time span of the initial lane's green signal, the system continually monitors traffic patterns within the other lanes. Should it detect a second high-intensity zone—indicative of heavy traffic in another lane—the signal for that particular lane shifts to yellow for a span of 4 seconds. Simultaneously, the two remaining lanes persist in displaying zero (red signal).
- Conclusion of the First Cycle: Post the initial 20 seconds, the green signal for the first lane concludes, marking the completion of the inaugural cycle. At this juncture, all lanes have undergone assessment, rendering the system poised to embark on the subsequent cycle informed by real-time traffic dynamics.
- Emergency Priority: In case of an exigency, the established cycle can be disrupted to accommodate priority instances. For instance, if an emergency vehicle necessitates unhindered passage, the system will bestow a green signal upon the lane occupied by the emergency vehicle, affording it safe traversal. Upon the resolution of the emergency, the system seamlessly reverts to its standard cycle, initiating from the initialization phase for all lanes.

The proposed system's modus operandi, characterized by dynamic adjustment of traffic signal timings in correspondence with detected traffic densities, underscores its potency in optimizing traffic flow and abating congestion. The elevated precedence accorded to high-intensity zones, coupled with the system's adaptability in handling exigencies, augments its efficiency and responsiveness in the face of fluctuating traffic conditions. By harnessing real-time image processing, the system exhibits the capacity to effect astute decisions aimed at ameliorating the comprehensive traffic management experience. This, in turn, engenders a more sustainable and efficient traffic control framework.

V. Conclusion

The envisaged strategy for the implementation of an intelligent traffic control system holds the potential to exert a substantial impact in ameliorating challenges such as traffic congestion, road accidents, and issues tied to traffic mismanagement. It is imperative to emphasize that this innovative approach necessitates no supplementary hardware installation; instead, it harnesses advanced image processing techniques to augment our preexisting system. A salient facet of this approach involves the adaptive adjustment of traffic signal timings in consonance with the discerned traffic density. The utilization of cutting-edge night vision cameras empowers the system to function optimally during diurnal as well as nocturnal conditions. The assimilation of such advanced systems into our existing infrastructure is poised to confer a noteworthy enhancement, ushering forth not only adept traffic management capabilities but also imparting a cadre of cost-effective solutions pertinent to traffic-related quandaries.

References

[1] C. Iftode, A. Zorilă, C. Vică, and E. Mihailov, "Experimental and relational authenticity: how neurotechnologies impact narrative identities," *Phenomenol. Cogn. Sci.*, Jun. 2022, doi: 10.1007/s11097-022-09825-7.

[2] M. W. M. Botes, "Brain Computer Interfaces and Human Rights: Brave new rights for a brave new world," in *2022 ACM Conference on Fairness, Accountability, and Transparency,* Seoul Republic of Korea: ACM, Jun. 2022, pp. 1154–1161. doi: 10.1145/3531146.3533176.

[3] D. Das and B. Semaan, "Collaborative Identity Decolonization as Reclaiming Narrative Agency: Identity Work of Bengali Communities on Quora," in *CHI Conference on Human Factors in Computing Systems,* New Orleans LA USA: ACM, Apr. 2022, pp. 1–23. doi: 10.1145/3491102.3517600.

[4] T. G. Mutambasere, "Diaspora citizenship in practice: identity, belonging and transnational civic activism amongst Zimbabweans in the UK," *J. Ethn. Migr. Stud.,* vol. 48, no. 3, pp. 732–749, Feb. 2022, doi: 10.1080/1369183X.2021.1916450.

[5] V. F. Reyna and C. J. Brainerd, "The importance of mathematics in health and human judgment: Numeracy, risk communication, and medical decision making," *Learn. Individ. Differ., 2007,* doi: 10.1016/j.lindif.2007.03.010.

[6] C. Srinivas et al., "Deep Transfer Learning Approaches in Performance Analysis of Brain Tumor Classification Using MRI Images," *J. Healthc. Eng.*, vol. 2022, pp. 1–17, Mar. 2022, doi: 10.1155/2022/3264367.

[7] J. Wu, P. Xiao, H. Huang, F. Gou, Z. Zhou, and Z. Dai, "An Artificial Intelligence Multiprocessing Scheme for the Diagnosis of Osteosarcoma MRI Images," *IEEE J. Biomed. Health Inform.*, vol. 26, no. 9, pp. 4656–4667, Sep. 2022, doi: 10.1109/JBHI.2022.3184930.

[8] A. Charidimou et al., "The Boston criteria version 2.0 for cerebral amyloid angiopathy: a multicentre, retrospective, MRI–neuropathology diagnostic accuracy study," *Lancet Neurol.*, vol. 21, no. 8, pp. 714–725, Aug. 2022, doi: 10.1016/S1474-4422(22)00208-3.

[9] C. S. Rao and K. Karunakara, "Efficient Detection and Classification of Brain Tumor using Kernel based SVM for MRI," *Multimed. Tools Appl.*, vol. 81, no. 5, pp. 7393–7417, Feb. 2022, doi: 10.1007/s11042-021-11821-z.

[10] R. E. Lucas, "On the mechanics of economic development," *J. Monet. Econ.*, 1988, doi: 10.1016/0304-3932(88)90168-7.

[11] H. Lund, "Renewable energy strategies for sustainable development," *Energy,* 2007, doi: 10.1016/j.energy.2006.10.017.

[12] M. Ikram, "Transition toward green economy: Technological Innovation's role in the fashion industry," *Curr. Opin. Green Sustain. Chem.*, vol. 37, p. 100657, Oct. 2022, doi: 10.1016/j.cogsc.2022.100657.

[13] M. Coccia, "Probability of discoveries between research fields to explain scientific and technological change," *Technol. Soc.*, vol. 68, p. 101874, Feb. 2022, doi: 10.1016/j.techsoc.2022.101874.

[14] "World Population Clock: 8 Billion People (LIVE, 2023) - Worldometer." https://www.worldometers.info/world-population/ (accessed May 30, 2023).

[15] "Trends in electric light-duty vehicles – Global EV Outlook 2023 – Analysis," *IEA.* https://www.iea.org/reports/global-ev-outlook-2023/trends-in- electric-light-duty-vehicles (accessed May 30, 2023).

[16] V. Jain, A. Sharma, and L. Subramanian, "Road traffic congestion in the developing world," in *Proceedings of the 2nd ACM Symposium on Computing for Development - ACM DEV '12,* 2012. doi: 10.1145/2160601.2160616.

[17] M. Sweet, "Does traffic congestion slow the economy?," *Journal of Planning Literature.* 2011. doi: 10.1177/0885412211409754.

[18] A. de Palma and R. Lindsey, "Traffic congestion pricing methodologies and technologies," *Transp. Res. Part C Emerg. Technol.,* 2011, doi: 10.1016/j.trc.2011.02.010.

[19] Md. A. Fattah, S. R. Morshed, and A.-A. Kafy, "Insights into the socio-economic impacts of traffic congestion in the port and industrial areas of Chittagong city, Bangladesh," *Transp. Eng.*, vol. 9, p. 100122, Sep. 2022, doi: 10.1016/j.treng.2022.100122.

[20] T. Bokaba, W. Doorsamy, and B. S. Paul, "A Comparative Study of Ensemble Models for Predicting Road Traffic Congestion," *Appl. Sci.*, vol. 12, no. 3, p. 1337, Jan. 2022, doi: 10.3390/app12031337.

[21] G. Cookson and B. Pishue, "INRIX Global Traffic Scorecard," *Inrix Glob. Traffic Scorec.*, 2017.

[22] United nation, "The Millenium Development Goals Report 2014," *U. N.*, 2014, doi: 10.1177/1757975909358250.

[23] C. Cai, C. K. Wong, and B. G. Heydecker, "Adaptive traffic signal control using approximate dynamic programming," *Transp. Res. Part C Emerg. Technol.*, 2009, doi: 10.1016/j.trc.2009.04.005.

[24] S. Maadi, S. Stein, J. Hong, and R. Murray-Smith, "Real-Time Adaptive Traffic Signal Control in a Connected and Automated Vehicle Environment: Optimisation of Signal Planning with Reinforcement Learning under Vehicle Speed Guidance," *Sensors,* vol. 22, no. 19, p. 7501, Oct. 2022, doi: 10.3390/s22197501.

[25] Md. A. Mondal and Z. Rehena, "Priority-Based Adaptive Traffic Signal Control System for Smart Cities," *SN Comput. Sci.*, vol. 3, no. 5, p. 417, Aug. 2022, doi: 10.1007/s42979-022-01316-5.

[26] R. M. Savithramma, R. Sumathi, and H. S. Sudhira, "A Comparative Analysis of Machine Learning Algorithms in Design Process of Adaptive Traffic Signal Control System," *J. Phys. Conf. Ser.*, vol. 2161, no. 1, p. 012054, Jan. 2022, doi: 10.1088/1742-6596/2161/1/012054.

[27] Z. Mo, W. Li, Y. Fu, K. Ruan, and X. Di, "CVLight: Decentralized learning for adaptive traffic signal control with connected vehicles," *Transp. Res. Part C Emerg. Technol.*, vol. 141, p. 103728, Aug. 2022, doi: 10.1016/j.trc.2022.103728.

[28] B. Van Arem, C. J. G. Van Driel, and R. Visser, "The impact of cooperative adaptive cruise control on traffic-flow characteristics," *IEEE Trans. Intell. Transp. Syst.*, 2006, doi: 10.1109/TITS.2006.884615.

[29] D. McKenney and T. White, "Distributed and adaptive traffic signal control within a realistic traffic simulation," *Eng. Appl. Artif. Intell.*, 2013, doi: 10.1016/j.engappai.2012.04.008.

[30] C. R. Lindsey and E. T. Verhoef, "Traffic Congestion and Congestion Pricing," in In: *Handbook of Transport Systems and Traffic Control (eds., Button KJ. and Hensher D.A.),* 2001. doi: 10.1093/brain/awg077.

[31] G. Padmavathi, D. Shanmugapriya, and M. Kalaivani, "A Study on Vehicle Detection and Tracking Using Wireless Sensor Networks," *Wirel. Sens.*

KIET

KARACHI INSTITUTE OF ECONOMICS AND TECHNOLOGY

Main Campus, PAF Base Korangi Creek

Tel: 35091114 - 7 | Cell: 0336-250284 - 85